THE ANALYSIS AND INTERPRETATION OF THE ANOMALIES TRANSITION IMPURITY DIFFUSION IN ALUMINIUM

A Thesis

Presented to The

School of Graduate Studies

and

The Faculty of Science

Addis Ababa University

In Partial Fulfillment of the

Requirements for the Degree

Master of Science in Physics

by

Yewondwossen Mammo

June, 1985

ACKNOWLEDGEMENTS

I am deeply most grateful to my beloved advisor and instructor, Prof. J.S Netchaev, whose exceptional talent and rich experience in the field, ever availability, encouragement and patience made this paper a reality in a very short time. In addition, I owe a dept to Dr. Netchaev for arising a strong interest in areas of applied physics related to materials science.

I should like to express my thanks to my academic colleagues at Kotobe College of Teacher Education, and particularly to Ato Gessese Tadesse and Ato Tesfaye Teshome for reading the manuscript and making many helpful corrections and Ato Kahsay Teka who shared my responsibilities during my studies.

I am particularly grateful to the Acquisition Department of Addis Ababa University Library for its cooperation.

I am also grateful to Ato Girma Dagne for his patience in assisting me in the technical preparation.

C O N T E N T S

LIST OF TABLES

LIST OF FIGURES

ABSTRACT

Analysis of the existing interpretations on the anomalous of transition impurity diffusion Aℓ is made. A synthesizing simple theoretical model is developed, assuming dislocations decorated by segregation phases, which made it possible to interpret the diffusion anomalies both quantitatively and qualitatively. Furthermore, the near-dislocation segregation regions structure and characteristics are studied from crystallography, thermodynamics of solids point of view and dislocation theory for adequate explanation of the anomalies.

CHAPTER I

INTRODUCTION

1.1 Definitions and Measurements of Diffusion Characteristics

Measurements of a diffusion process are usually expressed interms of the diffusion coefficient , the activation energy and the entropy or frequency factor, which are known as the diffusion characteristics.

1.1.1 Method of Measurements

Diffusion is the process by which matter is transported from one part of a system to another as a result of random atomic motions. Quantitative measurements of the rate at which a diffusion process occurs are usually expressed in terms of a diffusion coefficient. The diffusion coefficient is defined as the rate of transfer of the diffusing substance across unit area of a section, divided by the space gradient of concentration of the section ; or as the flux density of the substance at unit gradient of the concentration. Thus, if the rate of transfer per unit area of section is $\vec{J}$, and C the concentration of the diffusing substance, then.

$$\vec{J} = -D\vec{\nabla}C \ , \qquad (1.1a)$$

Confining attention to one dimension only, and if x denotes the space coordinate, then 1.1a becomes

$$J_x = -D\frac{\partial C}{\partial x} \qquad (1.1b)$$

Expression (1.1) is a definition of the diffusion coefficient D; and is usually referred to as Fick's first law of diffusion. In some cases, such as diffusion in dilute solutions (solutions of solute concentration no greater than about 1 to 2 %), D can reasonably be taken as constant, in others, such as diffusion in concentrated solutions, it depends very markedly on concentration.

Considerable number of works of different investigators have been concerned with experimental measurements of diffusion characteristics in face-centered cubic (f.c.c.) dilute metal solutions, There are a number of ways in which this can be achieved. The Radiotracer Method is commonly used in finding the distribution of an impurity element in a solid, in which the radioactive isotope of the impurity element is used. In this technique, a closed tube diffusion is carried out by plating a thin film of the diffusant radioactive onto the flat face of a metal-solvent slice, The film then becomes the diffusion source (solute), The metal slice is taken from tube at the end of diffusion, and a thin layer is removed from the surface. The radioactivity of the layer is counted and compared with that from a standard piece of the element. The amount of the impurity element in the layer can then be calculated, and if the dimensions of the layer are known, the mean concentration of the element in the layer can be found. Further layers are removed, and the

procedure is repeated, In this way the diffusion profile of the impurity in the metal is plotted.

The distribution of an impurity after diffusion can obey the "thin film" solution of the diffusion equation

$$C(x,t) = \frac{q_o}{S(\pi Dt)^{\frac{1}{2}}} \exp(-x^2/4Dt), \qquad (1.2)$$

where $C(x,t)$ is the concentration of tracer at a depth x from the cross-sectional area S after a diffusion time t, D is the tracer diffusion coefficient and q_o the quantity of tracer originally at the surface. The D values are calculated from the experimental plot of log C versus x^2.

Since diffusion occurs as a result of the random motion of particles, which are always thermally activated in solids the diffusion coefficient thus becomes a very strong function of temperature (T) and a relation of the form

$$D = D_o \exp(-Q/RT), \qquad (1.3)$$

is often followed, where the activation energy (Q) and frequency factor or entropy factor (D_o) for an impurity diffusion in the metal-solvent are derived from the linear plot of log D versus 1/T. The diffusion coefficient is then a constant at a constant temperature.

1.1.2 Types of Experimental Results

Measurements of the type discussed above have been made by many investigators for a large number of solutes (transition and nontransition metals) in Aluminium (Aℓ). There are several types of experimental results that are commonly drawn upon. Some of them are the following:

i) The so called "Impurity Diffusion Coefficient" denoted by D, describes the limiting diffusion rate of solute at extremely low concentration in the solvent. D nearly always has a simple Arrhenius type temperature dependence given by expression (1.3).

ii) D is always compared with D_s , the pure solvent self-diffusion (the diffusion of radioactively-labelled atoms of the solvent itself) coefficient. D for any solute may be either larger or smaller than the self-diffusion coefficient D_s , which also varies with T like (1.3)

$$D_s = D_{os} \exp(-Qs/RT), \qquad (1.4)$$

with activation energy Q_s and entropy or frequency factor D_{os}. The differences between D and D_s are related to changes in both the frequency factors (D_o, D_{os}) and the activation energies (Q, Q_s).

A significant feature is that the differences in activation energies,

$$\Delta Q = Q - Q_s , \qquad (1.5)$$

are sufficiently large to be the dominant influence in determining whether D is greater or less than D_s , so that it is about a theoretical interpretation of ΔQ that an understanding of the relative diffusion rates of solute and solvent largely hinges.

1.2 Formulation of the Diffusion Anomalies in Aℓ

Nontransition impurity diffusion in Aℓ shows normal diffusion rates and characteristics at high temperature, but transition impurity diffusion in Aℓ shows gross departures from normal solute diffusion rates and characteristics.

1.2.1 Nontransition Impurity Diffusion

At high temperature, close to the melting point (m.p.) of Aℓ , nontransition impurities revealed a pattern of behaviour that has come to be known as "normal impurity diffusion" with characteristics (D_o, Q, D). The essential feature of this is that D and D_s do not usually differ by more than about an order of magnitude at the m.p. The relative values of D and D_s are determined for the most part by expression (1.5). It is well known that the difference between the activation energies for impurity and self-diffusion (ΔQ) in Aℓ can be calculated theoretically by the LeClaire-Lazarus model, which yields a good agreement with the experimental data (Chapter 2).

Important among other defects present in real crystalline solids is dislocation. There are several basic types of dislocations. Two basic types of dislocations, edge and screw dislocations, are illustrated in Figure 1.

The most straightforward way that a dislocation can influence diffusion is to act as a "pipe" of high diffusivity, fast diffusion. This dislocation pipes can exhibit diffusivities greatly in excess of the surrounding lattice, and can therefore act as short-circuiting paths relative to lattice diffusion. The presence of such defects in the solvent produce enhanced diffusion at relatively low-temperatures in the case of nontransition impurities diffusion. The associated segregation towards dislocations, discussed by Cottrel and Nabarro which has come to be known as Cottrel cloud, can be due to elastic or electrical and chemical interactions due to the strain field of the dislocation. Such a fast diffusion could be explained satisfactorily using Hart-Mortlock theory which in turn employs the Cottrel cloud.

Nontransition impurity diffusion in Aℓ , with the two feasible results (normal and fast diffusion at high and relatively low temperatures, respectively) and their defining theories, is summarized in the chart below:

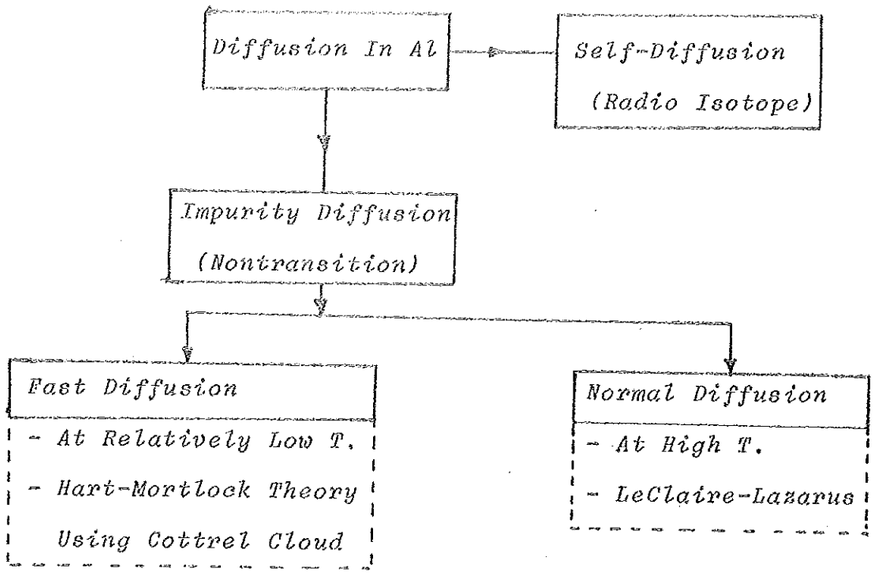

1.2.2 Transition Impurity Diffusion

Unlike the nontransition impurity diffusion case, many investigators on the diffusion of transition impurity in Aℓ have obtained low values of the diffusion coefficient while, a few, investigators have got normal diffusion coefficient values. According to the experimental data of some authors slow diffusion is exhibited with diffusion coefficient 1-4 orders less than the self-diffusion coefficient (D_s). The slow diffusion in turn is characterized by two groups: a series of tracer diffusion results in Aℓ characterized by anomalous low frequency factors and relatively low Q which have come to be known as "anomalous low"; and a series of tracer diffusion

results characterized by anomalously high activation energies and relatively high frequency factors which have come to be known as "anomalous high". Hence, transition impurity diffusion in Aℓ proceeds with anomalous high characteristics (D_o^* , Q^* , D^*), anomalous low characteristics ($D_{o\ell}^*$, Q_ℓ , D_ℓ) and normal (D_o , Q , D) values (close to the self-diffusion characteristics of Aℓ (D_{os}, Q_s, D_s)); where the relation $D_o^* >> D_{os} >> D_{o\ell}$, $Q^* > Q_s > Q_\ell$, $D_s > (D^*, D_\ell)$, $D_o \simeq D_{os}$, $Q \simeq Q_s$ and $D \simeq D_s$ holds.

In the 60's and 70's of this century there had been discussions in the leading journals (Physical Review, Acta Metallurgica, Philosophical Magazine, Journal of Applied Physics, Journal of Physical Society of Japan and etc.) of the world on the interpretation of the anomalies transition impurity diffusion experimental d[illegible]a. The discussion stopped, somehow, without any form of interpretation. So far no complete explanation of their diffusion mechanism has been found although several attempts have been made. But the normal diffusion result could be explained by self-diffusion vacancy mechanism like nontransition normal diffusion. For normal diffusion, the difference in the activation energies (ΔQ) . calculated by the LeClaire-Lazarus model , gave good agreement with the experimental data as in the nontransition impurity diffusion case.

The anomalies of transition impurity diffusion in Al could be formulated as follows (Chapter 3).

i) At the same high temperature in the same metal solvent (Al) the same impurity (transition metal) proceeds with three distinct characteristics.

ii) Two of the anomalies, Viz. High and Low, so far have not been explained theoretically, where as the normal diffusion is explained by LeClaire-Lazarus model.

The transition impurity diffusion in Al with the three possible experimental results, anomalous high, anomalous low and normal, is summarized in the chart below:

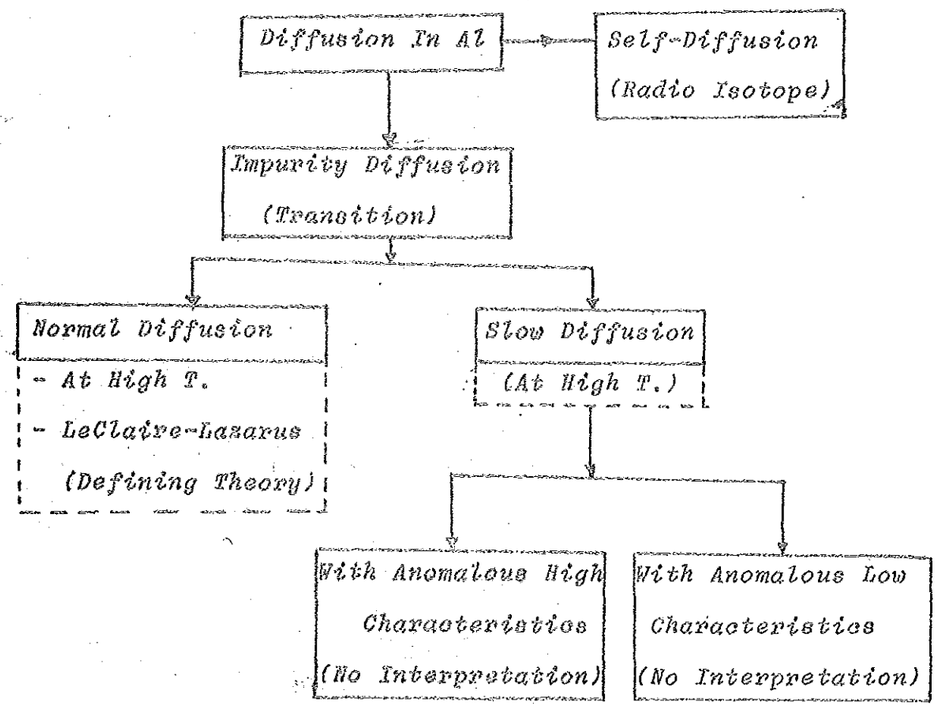

1.2.3 Experimental Inference

Quite a few number of normal diffusion results have been reported, but on the anomalous high and low characteristics numerous results have been reported. In the 60's the anomalous low results were believed to characterize true volume diffusion and had been published in metal hand books. Later on anomalous low and normal values were believed to be erroneous and anomalous high was thought to characterize true volume diffusion. Nowadays, the anomalous high values are given in metal hand books as true[1].

The presumption that the anomalous low characteristic values were due to systematic errors was shown to be groundless experimentally. Also, by reducing the dislocation density a shift from anomalous low to high characteristics was shown. It was concluded that the slow diffusion of an impurity in Al , in the near surface zone, proceeded with anomalous low characteristics because of the capture of the diffusing atoms by the dislocations in the near-surface zone. This capture of the impurity atoms leads to segregation of different forms. The attempt to employ the Hart-Mortlock theory together with Cottrel cloud to interprate the transition impurity diffusion anomalies has failed (Chapters 3 & 5).

From the analysis of the literature experimental data, in Chapter 3, the following conclusions are drawn:

i) The near-surface effect and the anomalous diffusion characteristics are caused by high dislocation density in the near-surface layers.

ii) Normal characteristics can be obtained when the dislocation influence is negligible.

iii) The anomalies of transition impurity diffusion in Aℓ are due to dislocations with segregation phases.

iv) The existing models of segregations on dislocations could not explain the diffusion anomalies.

1,3 Aims and Objectives

Transition metals are the most important components for many Aℓ alloys which are widely applied in modern technology (especially in aircraft and space ones). According to scientific predictions Aℓ alloys will have wide utilization in the future technology due to the relatively large stocks of Aℓ in the Earth.

For optimization of technological regimes of obtaining and thermotreatment of Aℓ alloys, it is necessary to know the mechanisms, models and true characteristics of the impurity diffusion in Aℓ.

The object of the present work is to

i) develope a synthesizing theoretical model based on the influence of dislocations decorated with segregation phases, and obtain fast, normal and slow diffusions as particular cases,

ii) develope the corresponding segregation model on dislocations, instead of Cottrel cloud and crystalline precipitate phases,

iii) demonstrate that the same anomalous behavior is shown by all transition impurities in Aℓ and thereby show the capacity of both the theory and segregation model to interprete the anomalies by taking iron (Fe) in Aℓ .

iv) predict the diffusion behavior.

1.4 Hypotheses

Based on the experimental data analysis the following hypotheses are framed to develop the theory and the segregation phase model. The hypotheses are proved theoretically.

1. Local equilibrium exists between the crystal region containing no dislocations (matrix) and the segregation phase regions along dislocations.

2. The impurity distribution law between the matrix solution and the segregation phase regions is linear.

Using this two conditions the effective diffusion coefficient is obtained in Chapter 4. From the interpretation it is found that anomalous low characteristics are obtained when diffusion proceeds along decorated dislocation with segregation phases, anomalous high characteristics are obtained when retarded volume diffusion attended by trapping of the impurity atoms prevail and normal characteristics characterize true volume diffusion when the dislocation influence is negligible. Treatment of the experimental data, using the developed theory, indicates some of the features of the segregation phase regions (Chapter 4). Consequently, the infeasibility to use the Cottrel cloud or crystalline precipitate phases is shown in Chapter 5.

3. The structure of the near-dislocation segregation phase regions is close to the structure of the corresponding intermetallic compound with some degree of amorphization.

Based on the third hypothesis, alternate microregions with high and relatively low degree of order are considered in the final chapter. Since the melting points of intermetallic compounds (for example $FeAl_3$) are higher than the m.p. of Al crystal and therefore much higher than the diffusion annealing temperatures, the secondary application of the Hart-Mortlock theory is made to interprate diffusion along decorated dislocations (low characteristics). Also, the structure of the segregation phase

regions and substantiation of the effective distribution law are promoted from crystallography and thermodynamics consideration using the dislocation theory.

In the subsequent chapters the diffusion of foreign atoms in a lattice is referred to as impurity diffusion. The diffusion of impurities which occupy normal lattice sites, i.e., where the impurities have simply replaced a certain number of atoms of the host lattice (Aℓ), which is known as substitutional impurity diffusion, is only discussed. In addition dilute solutions are considered.

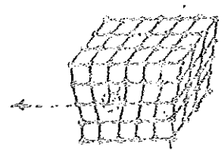

(a)

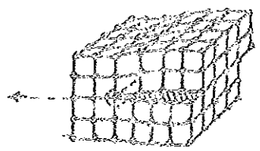

(b)

Fig.1. Two basic types of dislocations are illustrated.

a) The edge dislocation can be viewed as having been formed by slicing the crystal with a knife partway in from the top and inserting an extra half plane of atoms in the cut.

b) The screw dislocation could be produced by slicing partway in from the right and shearing the crystal parallel to the slice by one atomic spacing.

CHAPTER 2

NORMAL IMPURITY DIFFUSION IN DILUTE A% SOLUTION

In very dilute alloys solute atoms are sufficiently isolated from one another so that the interaction between them may be neglected and each atom can be regarded to diffuse nearly independently of the others. Theoretical treatment of the total diffusion then becomes simple. The expressions for diffusion properties can be written in terms of comparatively few but explicit and well defined solute and solvent jump frequencies and solute defect interaction energies. Such expressions are described and used in reviewing the general features of experimental results on diffusion in dilute alloys.

2.1 Properties of Normal Diffusion

By far the greatest amount of experimental information [2,3] comes from measurements of D_s and D, and extensive and systematic studies revealed normal impurity diffusion behavior. The important feature of normal diffusion being that D and D_s differ by less than an order of magnitude at the m.p., due to the comparatively small differences between Q and Q_s and between D_o and D_{os}. Roughly, $0.1 < D_o/D_{os} < 1$ and $0.8 < Q/Q_s < 1.1$, with smaller (larger) values of D_o tending to be associated with smaller (larger) values of Q.

For systems that are normal with respect to their diffusion characteristics, it is usually assumed, because of the small differences in properties, that the solute diffuses by the same vacancy mechanism that is so well established for self-

diffusion of the pure solvent.

The literature experimental data of self-diffusion (D_{OS}, Q_S, D_S) and some substitutional impurities diffusion (D_O, Q, D) characteristics in Al are given in Tables 1 and 2. As it can be seen in these tables, the normal diffusion regularities are valid for most of the impurities in Al except some transition impurities, Table 2.

2.1.1 Jump Frequencies Specification

If normal diffusion occurs by vacancies, all measured quantities can be expressed in terms of vacancy concentrations and vacancy jump frequencies. Fig.2 shows the "5-frequency model" commonly employed to discuss diffusion in dilute f.c.c. alloys. A solute atom is shown shaded. ω_2 is the jump frequency for a solute atom-vacancy exchange, unique when the solution is very dilute. Near to a solute atom solvent atoms may have jump frequencies which are different from the value ω_o characteristic of pure solvent: ω_1 is defined as the frequency for solvent-vacancy jumps between a pair of sites that are both nearest neighbours of a solute, ω_3 for vacancy jumps from 1st to more distant neighbour sites (2nd, 3rd, 4th) - "dissociative jumps" - and ω_4 for the reverse "associative jumps" onto 1st neighbour sites. All other solvent-vacancy jumps are assumed to occur with the frequency ω_o .

If ΔH_{sv} is the interaction energy (minus the binding energy)

of a solute atom with a nearest neighbour vacancy, the probability is $\exp[-(H_v + \Delta H_{sv})/RT]$ that a vacancy occurs on a particular site next to a solute atom, compared with the probability $\exp(-H_v/RT)$ of occurance on any other site. H_v is the vacancy formation energy in pure solvent. To maintain dynamic equilibrium between these vacancy concentrations demands the relation

$$\frac{\omega_4}{\omega_3} = \exp(-\Delta H_{sv}/RT) \qquad (2.1)$$

Each and every jump frequency has an arrhenius type temperature dependence with activation enthalpy H_i and pre-exponential factor ν_i, i.e.

$$\omega_i = \nu_i \exp(-H_i/RT) \qquad (2.2)$$

The activation entropy is contained in ν_i.

2.1.2 The Equation of ΔQ

As mentioned in Chapter 1, the differences between D_s and D are related to changes in the activation energies' (ΔQ). Attention has been given to try to account for the differences between D_o and D_{os} and between Q and Q_s instead of calculating D_o or Q directly. D is increasingly greater or less than D_s according as ΔQ is more negative or positive, respectively.

The pure solvent self-diffusion coefficient can be found to be

$$D_s = a^2 f_s \omega_o \exp(-H_v/RT) \quad , \qquad (2.3)$$

for f.c.c. metals, where a is the lattice parameter; f_s is the correlation factor for self-diffusion by vacancy mechanism, in this case a numerical constant equal to 0.7815 for f.c.c.

The equation for D, the impurity diffusion coefficient, is similar to (2.3) with ω_2 and f in place of ω_o and f_s and with ΔH_{sv} added into the vacancy concentration term,

$$D = a^2 f \omega_2 \exp[-(H_v + \Delta H_{sv})/RT] \quad , \qquad (2.4)$$

where, f is the correlation factor for impurity diffusion, is not merely a geometrical factor; ω_2 is the effective vibrational frequency of an impurity atom. Solvent jump frequencies enter into D through the correlation factor f. In simple case, like vacancy diffusion in isotropic crystals, f has the form[27]

$$f = \frac{u}{2\omega_2 + u} \quad , \qquad (2.5)$$

where u is a function of all the solvent jump frequencies. u has the expression

$$u = 2 \omega_1 + \omega_3 F(\omega_4/\omega_o) \quad , \qquad (2.6)$$

where

$$F(\infty) = 2 \; ; \quad F(1) = 5.15 \; ; \quad F(0) = 7$$

when $\omega_2 >> u$, f is small. This is because one solute jump is then highly likely to be followed by a second jump in the reverse direction. When $\omega_2 << u$, f is near unity. This is because the vacancy in this case makes many exchanges with solvent atoms after solute jump and so becomes near randomised in position with respect to the solute before the second jump.

From the definition of the experimental activation energy

$$Q = - R \frac{\partial \log D}{\partial (1/T)}$$

$$Q_s = - R \frac{\partial \log D_s}{\partial (1/T)} \qquad (2.7)$$

and equations (2.3) and (2.4) ΔQ is readily found to be

$$\Delta Q = Q - Q_s = \Delta H_2 - \Delta H_{sv} - C \quad , \qquad (2.8)$$

where $\Delta H_2 = H_2 - H_o$ and $C = R \, \partial \log f / \partial (1/T)$. f_s is constant but f will vary with T if the component frequencies have different activation energies. Usually C will be numerically smaller than $\Delta H_2 - \Delta H_{sv}$.

When C varies with temperature there is a corresponding variation of D_o, for this is easily seen to contain the factor $f_2 \exp(-C/RT)$, which is independent of temperature only when C is.

Equation (2.8) expresses the fact that solutes that attract vacancies (i.e. ΔH_{sv} positive) and also exchange with them

much more rapidly than do solvent atoms, so that $\omega_2 >> \omega_o$ (i.e ΔH_2 negative) , will have negative values of ΔQ and are therefore most likely to be fast diffusers.

2.2 LeClaire - Lazarus Model

To calculate ΔQ it is necessary to compute energy differences ΔH_{sv}, ΔH_2, etc. The only model from which ΔQ has been derived in a direct manner is using the well-known half vacancy electrostatic model [28,29] . This screening theory proposed by Lazarus [29] and used with considerable success by LeClaire [28] is also known as LeClaire-Lazarus model. This calculates ΔQ in terms of electronic properties and gives an immediate explanation of the correlation of ΔQ with vacancy that is observed in many systems. The energy of any configuration in the metal containing solute differs from that of an equivalent configuration in the pure metal only by a term due to the interaction between the vacancy and the screened effective charge difference between solute and solvent ion cores.

2.2.1 Thomas - Fermi Method

The screened interaction can be calculated in the Thomas-Fermi approximation. A free electron model is assumed for the pure metal with the positive ion cores smeared out to give a uniform positive charge density equal to the uniform negative electron density, Adding an impurity atom is regarded as replacing a solvent ion (of charge $Z_o e$) by an ion

carrying some different effective charge (of charge Z_2e). The difference in charge, $Ze = (Z_2-Zo)e$. is considered to be concentrated as a point charge situated at the centre of the impurity atom. Ze attracts electrons (if positive) or holes (if negative) so as to screen out the charge at large distances and the electrostatic potential due to it, $V(\gamma)$, is changed from $+ Ze/\gamma$ to a value which may be obtained as the solution of the Thomas-Fermi equation. The extra Z conduction electrons which enter with the solute atom go into the conduction band and maintain the Fermi-energy ε_F . constant, provided the concentration of solute is very small.

The Thomas-Fermi potential form, the leading term at a distance r from the excess point charge, can be given as[30]

$$V(\gamma) = \frac{Ze}{\gamma} \alpha \exp(-q\gamma) \quad , \qquad (2.9)$$

where α is a known function of Z 31 and of order unity and q is the "screening constant" given by $q^2 = 4\pi N(\varepsilon_F)$, $N(\varepsilon_F)$ is the density of states at ε_F.

The three terms in equation (2.8), Viz., ΔH_{sv}, ΔH_2 and C, can be extimated as follows:

ΔH_{sv}. A vacancy is usually regarded as an impurity with effective charge equal to $- Z_o e$ ($-3e$ in trivalent Aℓ). The change in the energy of formation ΔH_{sv} is assumed to be mainly to the electrostatic interaction between the vacancy and the impurity ion when they are nearest neighbors. The

nearest neighbor distance (nonbasal jump distance) is equal to a (see Fig.3). Then,

$$\Delta H_{sv} = Z_o eV(a) = 3eV(a) \ , \qquad (2.10)$$

$V(\gamma)$ is given by (2.9). The values of ΔH_{sv} are listed in Table 3.

ΔH_2. When an atom jumps from one sit to another it is the change in energy on passing from the equilibrium to the saddle-point configuration which determines the activation energy H. For the saddle-point configuration, it is assumed that the diffusing ion, situated midway between two equilibrium sites, is flanked by two half-vacancies whose charges are assumed to be centered at the centroids of the hemispheres (see Fig.3). Then, ΔH_2 is estimated as the difference in electrostatic interaction energies between the two charged each carrying effective charge of $-\frac{1}{2} Z_o e$ ($-3/2e$ for Aℓ), each situated at a distance $(11/16)^a$ from the impurity ion of effective charge Ze, and a charge $-Z_o e$ ($-3e$ for Aℓ) situated at a distance a from the impurity ion. Thus,

$$\Delta H_2 = -Z_o e \ V(11/16^a) + Z_o e \ V(a) \ . \qquad (2.11)$$

The last term is simply ΔH_{sv} , so that

$$\Delta H_2 - \Delta H_{sv} = - Z_o e \ V(11/16^a) . \qquad (2.12)$$

The value of ΔH_2 are listed in Table 3.

C. The expression for impurity diffusion correlation factor, in fair approximation, is given by [32]

$$f = \frac{\omega_1 + 7/2\ \omega_3}{\omega_1+\omega_2+7/2\ \omega_3} \qquad (2.13)$$

where ω_i is given by eq.(2.2). Differentiating Eq.(2.13) to give C leads to an expression which is easily thrown into a form containing only the differences in activation energy $\Delta H_i = H_i - H_o$, and the ratios of the frequency terms, ν_i/ν_o. A value for the ratio ν_2/ν_o can be found by equating the theoretical and experimental values for the ratio D/D_s. This leads, using Eq.(2.8), to

$$\frac{\nu_2}{\nu_o} = \left(\frac{D_o f_s}{D_{os} f} \right) \exp\ (C/RT) \ . \qquad (2.14)$$

No corresponding expressions can be found for ν_1/ν_o and ν_3/ν_o , but since these frequencies all refer to variations of the same atomic species, it is possible to assume that the ratios are both equal to one. The expression for C then reduces to the equation,

$$C = \frac{D_o}{D_{os}}\ f_s \exp(C/RT) \quad x$$

$$\left\{\frac{(\Delta H_2-\Delta H_1)\exp\left[-(\Delta H_2+\Delta H_1)/RT\right]+\frac{7}{2}(\Delta H_2-\Delta H_3)\exp\left[-(\Delta H_2-\Delta H_3)/RT\right]}{\exp\left[-\Delta H_1/RT\right]+\frac{7}{2}\exp\left[-\Delta H_3/RT\right]}\right\}^2 \qquad (2.15)$$

The values of ΔH_1 and ΔH_3 can be estimated by analogy, i.e, by considering the saddle point configuration. The calculation of the correlation correction C is then obtained by solution of Eq.(2.15) after substituting it by the estimated values of D_o and D_{os} .

For positive Z impurities ΔH_{sv} and ΔH_2 are positive and negative, respectively: they attract vacancies and there is a reduction of the saddle point energy of their jumps relative to that for pure solvent atom jumps. C also turns out to be negative in this case [28] but appreciably less numerically than the difference $\Delta H_2 - \Delta H_{sv}$, so that ΔQ is negative. These are precisely the properties of completely normal impurity diffusion.

Table 3 shows some values of ΔQ calculated from the model. It is, however, well known that the Thomas-Fermi equation (2.9) is a rather rough approximation to $V(\gamma)$ and that more accurate expressions are available. These are based on the Hartree equation and have been developed by Kohn and Vosko, Friedel, March and others [33-39]. They do not differ much from the Thomas-Fermi potentials at short distances but have important and highly significant property of becoming oscillatory at larger distances: the differences here are therefore profound.

Now at least for monovalent metals it turns out that the distances of interest in a calculation of ΔQ are comfortably within the region where the potentials are similar, so it matters little which potential is used: both give similar values of ΔQ [40]. However, for polyvalent metals, on account of their higher electron density, the oscillations become effective at nearest neighbour distances or less and so have a profound influence on the value of ΔQ . In particular,

with possible changes now in the sign of $V(\gamma)$ in the relevent range of γ, there is no reason always to expect for solutes in polyvalent solvents the same simple dependent of ΔQ on valence that one finds for normal monvalent solvents.

It is perhaps surprising, in view of these remarks, that a normal valency dependence is not found in Aℓ, for which the data, as shown in Table 3, are particularly extensive. All the nontransition solutes show normal (diffusion in that D_o and Q differ little from D_{os} and Q_s, but ΔQ remains comparatively small and shows no obvious dependence on the valency difference, despite this variation all the way from -2 to +2. The other interesting feature is that the transition period solutes show unusually large values of Q and D_o, although D and D_s still differ comparatively little near the melting point.

2.2.2 Oscillatory Type Potential

It is well known that the difference between the activation energies for impurity and self-diffusion in noble metals can be interpreted by the LeClaire-Lazarus model containing the electrostatic shielding around the impurity in Thomas-Fermi approximation. In polyvalent metals, however, theoretical calculations based on the above approximation yielded bad agreement with the experimental data (see eg.[6]). It is reasonable to suppose that in metals having higher valency, the Thomas-Fermi model, leading to an exponential dependence of the shielding potential on the distance from the impurity, is a very crude approximation even for first neighbours. As

was shown by theoretical calculations [34,35] and by experimental nuclear magnetic reasonance (NMR) investigations, the excess potential around impurities has an oscillational character even in noble metals. It can be expected that the shielding will be stronger in Aℓ because of the larger electron density, and the oscillations will occur closer to the impurity.

For a few impurities in Aℓ, calculations have been made [21,10] of ΔQ that recognise the need to use a more correct oscillatory type of potential for V(r). The results of these calculations (Tables 4 and 5) are in reasonable agreement in sign and magnitude for some nontransition impurities. It is interesting to note that the sign and magnitude of ΔQ theoretical (ΔQ_{Th}) and ΔQ experimental (ΔQ_{Exp}) depend on the choice of the experimental values of the characteristics of impurity and self-diffusion (Table 4) and usually coincide in order of magnitude with scattering of the experimental data on Q and Q_s obtained by different authors (Table 1). Therefore the quantitative comparison of ΔQ_{Th} and ΔQ_{Exp} is rather difficult.

In the calculation of Q 21,10 the asymptotic form for V( ) employed,

$$V(\gamma) = \frac{\alpha_o |e|}{4\pi K_F^2} \quad \frac{\cos(2K_F\gamma+\phi)}{\gamma^3} \quad , \qquad (2.16)$$

which is valied only for large γ [36]. K_F is the Fermi wave vector for the solvent (Aℓ), α_o a constant and ϕ the phase

factor. The value of α_o and ϕ can be estimated from electrical resistance or NMR measurements.

The simple half-vacancy electrostatic model seems to provide a satisfactory qualitative, and in many respects quantitative, description of the main features of normal impurity diffusion in spite of its obvious shortcomings. At the same time this model is based on rough assumptions which is necessary to exclude in more better models, Viz.: treating the impurities, vacancies and half-vacancies as effective point charges; neglecting the size factor (differences in atomic radii) and lattice relaxation ; and employing the free electron (sommerfeld) in the derivation of the expressions for $V(\gamma)$ and so on. Analysing the experimental and theoretical values of ΔH_{sv} and ΔQ_{Th} for Cu, Ag, Zn, Ge, Sb in Al, obtained in the framework of the electrostatic model of halfvacancies using both types of potentials (expressions (2.9) and (2.16)), Peterson and Rothman [6] came to the conclusion that the original modification of the electrostatic [29] (Lazarus) gave more satisfactory agreement with experiment. The authors noted also that the consideration in the framework of the Swallin theory [40] of the size effect on ΔQ arising from the difference of atomic radii of the impurity and the solvent did not describe the experiment although there was some correlation between relative values of the impurity diffusion coefficients and the influence of the impurities on the lattice parameter of the matrix.

2.2.3 Other Attempts

While there has been considerable effort over the last two decades or more to develop more satisfactory theoretical description of vacancy-solute interactions (for calculation of ΔH_{sv}), for instance [33,45] , very less attention has been given to treating the saddle point configuration in a more realistic way for calculating the ΔH_1. Among the few efforts in this direction, it is necessary to mark the work [46] in which the value of ΔQ was estimated using the point charge model and self-consistant potential of the Hartree type that avoided reference to half-vacancies. ΔH_2 and C were found to be appreciably smaller and ΔH_{sv} rather larger than derived by the crude model [28] , the net result for ΔQ being in rather less good agreement with experiment.

More recently, pseudopotential methods have begun to be applied to calculating the migration energies [47,48] , but there seem so far to be no results sufficiently complete for direct comparison with experiment. Using the pseudopotential method the values of ΔQ for diffusion of Cd and Zn in Aℓ were obtained which are close to the experimental values. But the value of ΔQ for Mg in Aℓ , calculated by this method [49] , differs from the experimental values in sign and magnitude.

2.3 Correlation Between Frequency Factor and Activation Energy

Solute diffusion indicates that a correlation exists between the frequency factor D_o and the activation energy Q in a given solvent. Therefore, it is expedient to consider the correlation between the experimental characteristics (D_o and Q), of diffusion of substitutional impurities in Aℓ , for more accurate definition and expansive of the emperical relationships of the normal diffusion.

The correlation between $D_o(D_{os})$ and $Q(Q_s)$ can be described by [50].

$$D_o = A \exp(Q/RT_o) \quad , \qquad (2,17)$$

where A and T_o are the corresponding constants for the metal-solvent (Aℓ) , which can be found from the graph of log D_o versus Q (Fig.4) drawn based on the experimental data (Tables 1 and 2). For normal diffusion of substitutional impurities and self-diffusion of Aℓ , the following values of A and T_o were obtained:

$$A = (3.66 \ {}^{+37.8}_{-\ 3.35}) \times 10^{-8} \ \ cm^2/s$$

$$T_o = (9.26 \ {}^{+167}_{-123}) \ \ K$$

The observed correlation between D_o and Q can be explained on the basis of the electrostatic model [29] . Using the

Thomas-Fermi potential it is possible to obtain the following correlation due to Swallin 51 :

$$\frac{d\ell ogD_o}{dQ} = \left(\frac{\alpha}{2.3R}\right)\left\{\frac{(q\gamma_o+1)C/4(-q^3\gamma_o^3+6q^2\gamma_o^2+5q\ \gamma_o+5)}{|1-1/4(q^2\gamma_o-5q\gamma_o-5)|}\right\} \qquad (2.18)$$

where α represents the thermal expansion coefficient for the metal-solvent , R is the gas constant, γ_o the inter-atomic distance in the lattice of the metal-solvent, q the screening constant, C is a constant equal to about 3.

For A : $\alpha = 2.56\times10^{-5}K^{-1}$; γ_o=2.86A,[52] ; q=2.06$(A)^{-1}$,[29];

substitution in eq.(2.18) gives

$$\frac{d\ell ogD_o}{dQ} = 0.12 \text{ mole/KJ}$$

From expression (2.17) it follows that

$$\frac{d\ell ogD_o}{dQ} = \frac{1}{RT_o} \quad . \qquad (2.19)$$

Comparing (2.18) and (2.19) it follows that

$$T_o = 1000\ K$$

in satisfactory agreement with the experimental value (Fig.4)

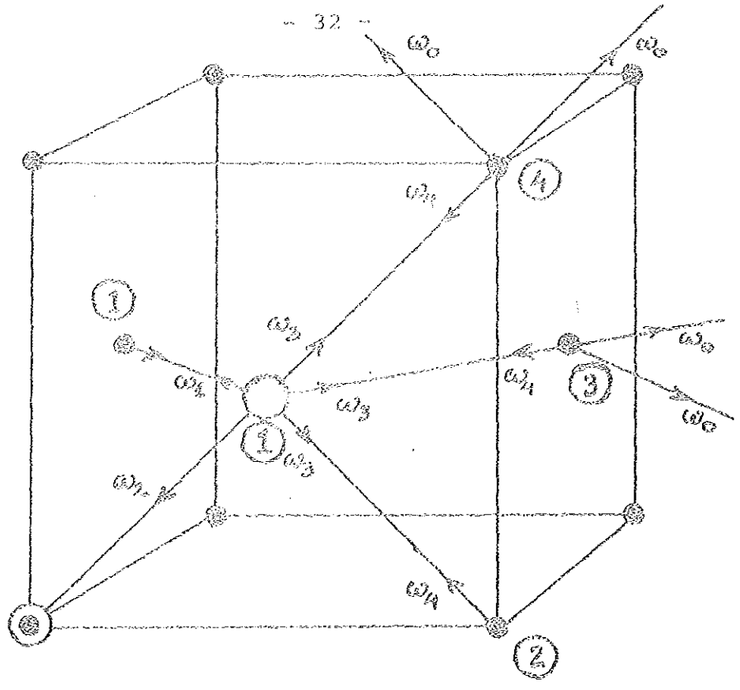

Fig 2. Frequencies ω_i for vacancy-atom jumps in f.c.c crystals. the arrows indicate the vacancy moves. The circled numbers indicate the order of neighbours to the solute atom at the origin.

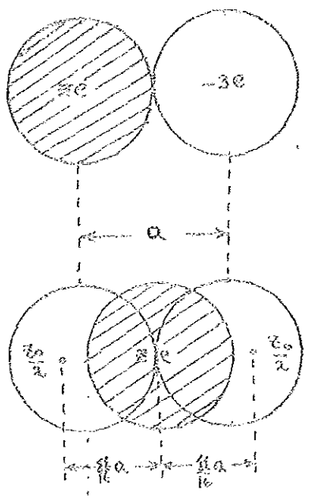

$Z_0 = +3e$ for Al

Fig 3. Diffusing ion and the vacancy in a)the equilibrium configuration and b) in saddle point configuration.

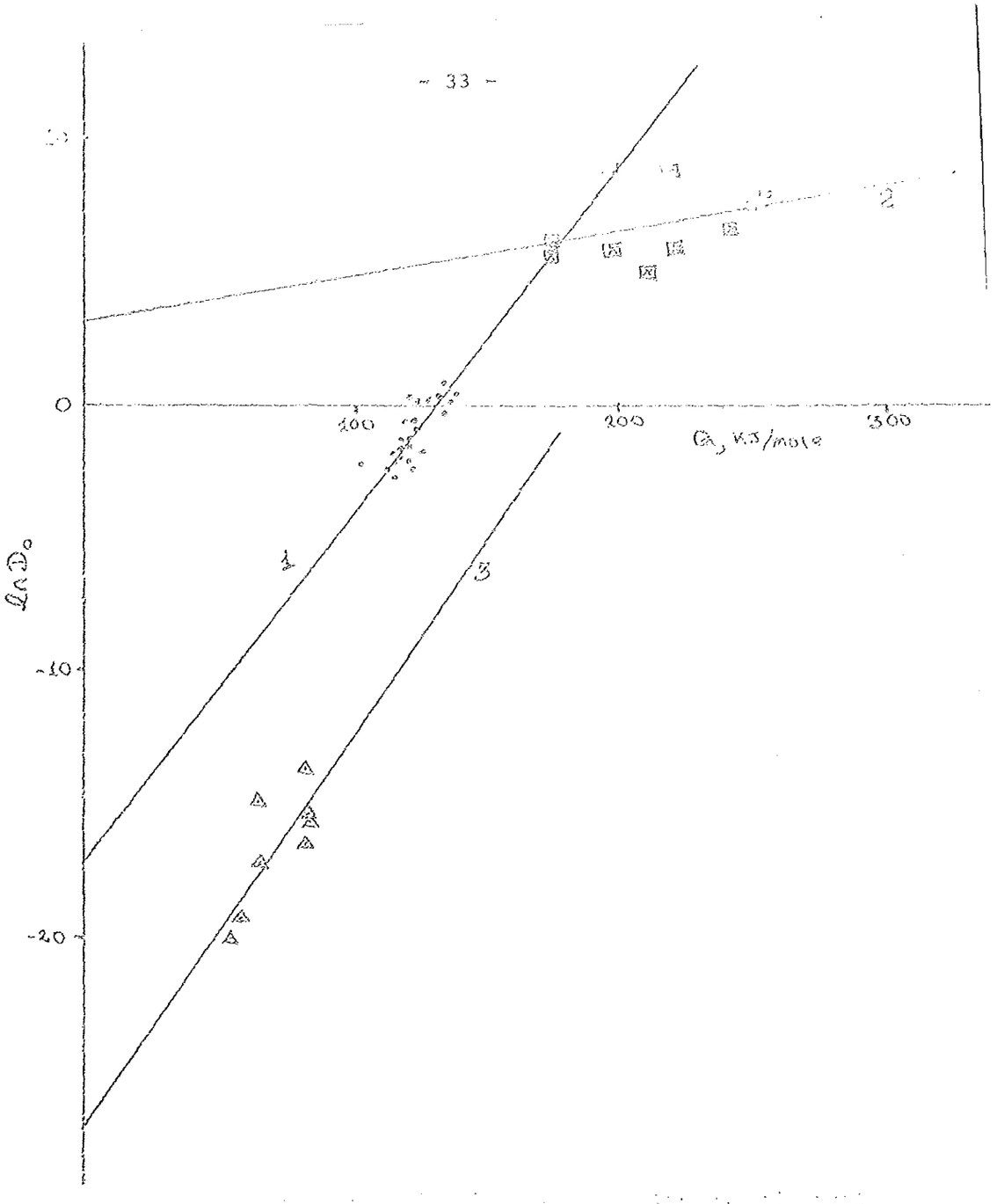
0
-10
-20
100
200
300
Ea, KJ/mole
ln D₀
1
2
3

Table 1

Characteristics of Self-and Impurity (Nontransition metals) Diffusion of Radioactive Isotopes in Al

Isotope	$D_o X10^{-4}$ m^2/S	KJ/mole	$D_{m.p.} X10^{-4}$ m^3/S	$(D/D_s)m.p.$	References
Al	2.25	145	$1.70x10^{-8}$		4
Al	1.71	142.3	$1.90x10^{-8}$		5
Al	0.11	121.4	$1.87x10^{-8}$	1	6
Cu	0.65	135.2	$1.82x10^{-8}$	0.97	6
Cu	0.15	126.0	$1.34x10^{-8}$	0.71	7
Ag	0.12	116.4	$3.88x10^{-8}$	2.07	6
Ag	0.13	117.0	$3.69x10^{-8}$	1.97	8
Au	0.13	116.4	$4.20x10^{-8}$	2.25	6
Au	2.20	134.0	$6.99x10^{-8}$	3.74	9,10
Au	0.08	113.0	$3.81x10^{-8}$	2.03	8
Mg	1.24	132.0	$5.10x10^{-8}$	2.73	11
Mg	0.10	121.4	$1.70x10^{-8}$	0 91	9
Cd	1.04	124.3	$1.20x10^{-7}$	6.41	8
Ga	0.49	122.2	$7.31x10^{-8}$	3.91	6
In	1.16	122.2	$1.73x10^{-7}$	9.25	12
Zn	1.10	129.4	$6.66x10^{-8}$	3.56	13
Zn	0.26	121.0	$4.41x10^{-8}$	2.36	6
Si	0.35	124.0	$4.04x10^{-8}$	2.16	14
Si	2.48	137.0	$5.36x10^{-8}$	2.86	9,10
Ge	0.48	121.4	$8.15x10^{-8}$	4.36	6
Sn	0.25	119.3	$5.49x10^{-8}$	2.94	15
Sb	0.09	122.0	$1.34x10^{-8}$	0.72	16
Mg	0.062	115.0	$2.29x10^{-8}$	1.22	10
Cu	1.30	138.0	$2.47x10^{-8}$	1.32	10
Zn	0.177	118.0	$4.42x10^{-8}$	2.36	10

Table 2

Characteristics of Self-and Impurity (Transition Metals) Diffusion of Radioactive Isotopes in Al

Isotope	T, K	$D_o x10^{-4}$ m^2/S	Q, KJ/mole	$D_{m.p.} x10^{-4}$ m^2/S	$(D/D_s)_{m.p.}$	References
Al		0.11	121.4	$1.87x10^{-8}$	1.0	6
Mn^{54}	729-916	0.22	120.6	$3.73x10^{-8}$	2.0	6
$Mn^{55;56}$	733-933	104	211	$1.62x10^{-10}$	$8.7x10^{-3}$	17
Mn	773-918	380	221.5	$1.53x10^{-10}$	$8.2x10^{-3}$	18
Fe^{59}	853-933	$9.1x10^{5}$	257.5	$3.33x10^{-9}$	0.18	19
Fe^{59}	791.5-898	$5.9x10^{3}$	220	$2.84x10^{-9}$	0.15	19
Fe^{59}	823-908.5	324	198	$2.14x10^{-9}$	0.14	8
Fe^{59}	632-903	$4.1x10^{-9}$	58.2	$2.27x10^{-12}$	$1.2x10^{-4}$	20
Cr^{51}	773-918	$2.4x10^{3}$	255.4	$1.29x10^{-11}$	$6.9x10^{-4}$	18,19
Cr^{51}	859-923	$1.8x10^{3}$	251	$1.63x10^{-11}$	$8.7x10^{-4}$	6,9
Cr^{51}	523-878	$3.01x10^{-7}$	64.5	$7.41x10^{-11}$	$4.0x10^{-3}$	20
Co^{60}	695-927	464	174.6	$7.89x10^{-8}$	4.2	6
Co^{60}	673-913	250	174.6	$4.25x10^{-8}$	2.3	21
Co^{60}	843-923	$7.21x10^{3}$	197	$6.84x10^{-8}$	3.7	22
Co^{60}	632-903	$1.1x10^{-6}$	83.3	$2.40x10^{-11}$	$1.3x10^{-3}$	20
Zr^{95}	804-913	728	242	$7.48x10^{-12}$	$4.0x10^{-4}$	9
Ni^{63}	632-903	$2.9x10^{-8}$	65.7	$6.11x10^{-12}$	$3.3x10^{-4}$	20
V^{48}	673-903	$6.05x10^{-8}$	82.1	$1.54x10^{-12}$	$8.2x10^{-5}$	23
Pd^{103}	673-903	$1.9x10^{-7}$	83.7	$3.94x10^{-12}$	$2.1x10^{-4}$	24
Mo^{99}	673-903	$1.0x10^{-9}$	54.4	$9.04x10^{-13}$	$4.8x10^{-5}$	25
Nb^{95}	673-903	$1.7x10^{-7}$	83.7	$3.52x10^{-12}$	$1.9x10^{-4}$	26

Table 3

Theoretical [21] and Experimental Values of ΔQ for Impurity (Nontransition) Diffusion in Al (Q_s=121.4 KJ/mole [6])

Impurity	Z_2-Z_o	H_{BV} KJ/mole	H_2, KJ/mole	C, KJ/mole	$\Delta Q_{Theo.}$, KJ/mole	$\Delta Q_{Exp.}$, KJ/mole	Refs.
Cu		1.9	6.7	∿0	+4.8	+13.8	6
Ag	-2	-6.4	-25.7	-14.5	-4.8	- 5.0	6
Au		-6.4			-4.8	- 5.0	6
Mg		4.3	17.7	∿0	+13.4	+10.5	11
Zn	-1	2.7	11.1	∿0	+ 8.4	+ 8.0	13
Zn						- 0.4	6
Cd						+ 2.9	8
Ga	0					+ 0.8	6
In						+ 0.8	12
Si						+ 2.5	14
Ge	+1	-10.1	-39.1	-26.0	-3.0	0	6
Sn						-2.1	15
Sb	+2					+0.6	16

Table 4

Theoretical [10] and Experimental Values of ΔQ for Impurity (Nontransition) Diffusion in Al (Potential Eq (2.9))

Characteristic KJ/mole	Ag	Au	Cu	Mg	Zn	Ca	Si
H_{Bv}	-9.7	-20.3	-9.1	-1.7	-1.8	-7.4	-13.5
H_2	-40.6	-84.0	-36.7	-6.9	-7.4	-29.9	-14.5
C (for 773 K)	-10.6[a,c]	-59.9[a,h]	-17.4[a,h]	-0.2[a,h]	-0.2[2,h]	-10.6[a,f]	-3.9[a,h]
	-29.9[b,c]	-83.1[b,h]	-37.7[b,h]	-2.0[b,h]	-5.1[b,h]	-29.0[b,f]	-19.3[b,h]
	-43.5[a,b]	-14.5[a,e]					-0.9[a,g]
	-65.7[b,e]						-10.6[b,g]
ΔQ_{Theo} (773 K)	-20.3[a,c]	-3.8[a,h]	-10.2[a,h]	-5.1[a,h]	-5.4[a,h]	-11.9[a,f]	-2.9[a,h]
	-1.0[b,c]	-19.4[b,h]	+10.1[b,h]	-3.2[b,h]	-0.5[b,h]	6.5[b,f]	18.3[b,h]
		-20.2[a,d]	-13.1[a,e]				-0.1[a,g]
		2.0[b,d]	6.2[b,e]				9.6[b,g]
ΔQ_{Exp}	-28.4[a,c]	-10.6[a,h]	-6.8[a,h]	-29.9[a,h]	-27.1[a,h]	-20.6[a,f]	-7.7[a,h]
	-6.2[b,c]	11.6[b,h]	15.4[a,h]	-7.9[b.h]	-4.9[b,h]	1.6[b,f]	14.5[b,h]
		-28.5[a,d]	-9.8[a,e]				-21.3[a,g]
		-6.3[b,d]	12.4[b,e]				0.9[b,g]

a) They used $D_{os} = 2.25 \times 10^{-4} m^2/S$; $Q_S = 144.9$ KJ/mole [5]
b) $D_{os} = 4.5 \times 10^{-6} m^2/S$; $Q_S = 122.7$ KJ/mole [41]
c) D_o(Au) $= 1.31 \times 10^{-5} m^2/S$; $Q = 116.5$ KJ/mole [6]
d) D_o(Au) $= 1.31 \times 10^{-5} m^2/S$; $Q = 116.4$ KJ/mole [6]
e) D_o (Cu) $= 6.47 \times 10^{-5} m^2/S$; $Q = 135.1$ KJ/mole [6]
f) D_o(Cd) $= 1.04 \times 10^{-4} m^2/S$; $Q = 124.3$ KJ/mole [8]
g) D_o(Si) $= 3.46 \times 10^{-5} m^2/S$; $Q = 123.6$ KJ/mole [44]
h) They used experimental values of D_o or Q [10]

TABLE 5

Comparison of Theoretical (Potential Eq. (2.9)) [19,21] and Experimental Values of ΔQ for Impurity (Transition Metals) Diffusion in Al. (Qs = 121.4 KJ/mole, [6])

Impurity	ΔH_{BV} KJ/mole	ΔH_2, KJ/mole	C, KJ/mole	$Q_{Theo.}$, KJ/mole	$Q_{Exp.}$, KJ/mole
					136 [19]
					99 [19]
					77 [8]
Fe	37	150	0	113	-63 [20]
					38 [42]
					42 [43]
					14 [44]
					53 [21,6]
Cr	27	112	0	85	76 [22]
					-38 [20]
					134 [9,8]
Cr	54	2)1	0	147	130 [6,9]
					-56.5[20]
					1 [5]
Mn	38	140	0	102	90 [17]
					100 [18]

CHAPTER 3

NORMAL AND ANOMALOUS DIFFUSION OF TRANSITION IMPURITY IN Aℓ

The experimental results and proposed interpretations of different investigators, and their methods and conditions of getting the anomalous characteristics of transition impurity diffusion in Aℓ are analyzed. These analyses have laid the foundations of the assumed hypotheses and synthesizing theoretical model developed in the next chapter.

3.1 The Experimental Results

The relation between normal and self-diffusion characteristics, described in section 2.1, could be violated when transition metals diffuse in Aℓ (Table 2). According to the data of some experimentors (Table 2), the diffusion characteristics (D_o, Q) of transition impurity in Aℓ could deviate from the self-diffusion characteristics, anomalous high and low characteristics. However, the diffusion characteristics could also remain close to the self-diffusion characteristics, normal characteristics.

3.1.1 Anomalous High Values

The values obtained [6-9, 17-19] when Fe, Mn, Cr and Zn diffuse in Aℓ could be attributed to anomalous high characteristics D_o^* and Q^*. The values of D^* for these impurities in Aℓ exceed the self-diffusion values, D_{os}, of Aℓ [4,5,6] by about (3-5) orders. The Q^* values were obtained to exceed

Q_s of Aℓ [4,5,6] by about 1.5 to 2 times. Accordingly, the diffusion coefficients D^* [6-9, 17-19] , at high temperatures, were less than the self-diffusion coefficients (D_s) [4,5,6] by about (1-3) orders.

The correlation between D_o^* and Q^* can be described by Eq.(2.17) with constants A^* and T_o^* . These constants, determined from Fig.4 line 2, are different from the normal diffusion constants A and T_o, Viz.

$$A^* = (22.2\ ^{+68.4}_{-21.5})\ \text{cm}/\text{S}\ ,\quad T_o^* = (7070^{+113000}_{-34400})\text{K}$$

If the C_Q data is excluded

$$A^* = (0.245^{+59,8}_{-0.244})\ \text{cm}/\text{S}\ ,\quad T_o^* = (3386^{+7067}_{-1366})\text{K}$$

3.1.2 Anomalous Low Values

When transition impurities diffused in the near-surface strata (depth, about 1-10μm) of polycrystalline Aℓ, at temperatures, the anomalous low values of the activation energy (Q_ℓ), the frequency factor ($D_{o\ell}$) and the diffusion coefficient (D_ℓ) were obtained [20,23-26] . For instance, the values of $D_{o\ell}$ (Table 2), for diffusion of transition metal isotopes (Fe, Ni, Co, Cr, V , Pd, Mo Nb) in the near-surface strata of A polycrystals, were lower than D_{os} [4,5,6] by about (5-8) orders. The authors [20,23-26] obtained the values of Qℓ (Table 2) to be 1.5 to 2 times

lower than Q_s, and the values of D_ℓ at high temperatures (Table 2) to be less than D_s [4,5,6] by about (2-4) orders.

The results listed in Table 2 indicates that the normal and self-diffusion relation are violated when the diffusion proceeds with anomalous low characteristics ($D_{o\ell}$, Q_ℓ, D_ℓ) (see Fig.4).

The correlation between $D_{o\ell}$ and Q_ℓ could be described by Eq.(2.17) with different constants. These constants, which are different from the normal diffusion, could be found from Fig.4 line 3, Viz.

$$A_\ell = (1.58^{+46.6}_{-1.53})\times10^{-12}\ cm^2/S\ ,\ T_o = (830^{+390}_{-200})K$$

The values of the constants $T_{o\ell}$ and T_o coincide within their errors of determination. However, the difference between the values of Aℓ and A is much larger than the errors of their findings. The ratio A_ℓ/A reaches about 4×10^{-5}, i.e. there is spasmodic change of the A parameter and corresponding spasmodic change of the log D_o and Q dependence (Fig.4).

3.1.3 Normal Values

The results of Lundy and Murdock [5] could be sighted as a typical example in which normal characteristics were obtained (Table 2). According to the authors result [5] Mn diffused in Aℓ with normal characteristics (D_o=0.22 cm^2/S, Q = 121 KJ/mole, $(D/Ds)_{M.p}$ = 2.0).

For Mn diffusion in Aℓ, however, there is a very large discrepancy between Hood and Shultz, Fricke's [17,18] findings and the Mn^{56} tracer studies of Lundy and Murdock [5] . According to the results of the authors [17,18] Mn diffused in Aℓ with anomalous high characteristics: $D_o^* = 1.04 \times 10^2$ cm²/S, $Q^* = 211$ KJ/mole, $(D^*/Ds)M.p = 8.7 \times 10^{-3}$ [17] ; $D_o^* = 3.8 \times 10^2$ cm²/S, $Q^* = 221.5$ KJ/mole, $(D^*/Ds)M.p = 8.2 \times 10^{-3}$, [18] ; (Table 2).

Normal diffusion characteristics of Fe in Aℓ [42,43,44] were obtained by indirect methods. For instance in [44] they studied the dynamical properties of Fe^{57} isotope by the Mossbauer technique, which was dissolved in Aℓ lattice, with a quantity of about 10^{-7} atomic fraction. The diffusion characteristics of Fe in dilute Aℓ-solution obtained using this technique ($D_o = 0.1$ cm²/S, $Q = 135$ KJ/mole, $(D/Ds)M.p = 0.18$;[44]) were, relatively, close to the self-diffusion characteristics of Aℓ ($D_{os} = 0.1$ cm²/S, $Qs = 121.4$ KJ/mole; [6]). It is worthy to mention that this method [44] assumed some rough approximations to obtain the diffusion characteristics from the Mossbauer data.

On the other hand, in different works [42,43] the kinetic of the decomposition of supersaturated solutions of Fe in Aℓ was studied by Mossbauer and resistometric technique. It was shown that the diffusion of Fe in Aℓ solution,

during the stage of the growth of the second phase particle proceeded with activation energies (Q = 161±7 KJ/mole, [43]; Q = 159±2 KJ/mole, [42]) which was, relatively, close to the self-diffusion activation energy (Q_s = 145 KJ/mole, [4]; Q_s = 142 KJ/mole, [5] ; Q_s = 121,4 KJ/mole, [6]).

It is possible to show that the calculation of the activation energy of "normal" diffusion of Fe in Aℓ lattice using the Thomas-Fermi potential, carried out within the framework of LeClaire-Lazarus model [28,29] , gives a value of about 159 KJ/mole which coincide with the experimental values of Q [42,43] . In calculating Q, the effective charge of the impurity (Z_{Fe}-$Z_{Aℓ}$) was taken to be minus unity [53] and the self-diffusion activation energy of Aℓ was taken to be 121,4 KJ/mole [6] .

The diffusion characteristics of the third group correspond to normal correlation between D_o and Q which could be described by Eq.2,17. The same constants, A and T_o, as for nontransition substitutional impurities can be found (Fig.4 line 1).

In particular for normal diffusion Fe in Aℓ , the value of Do which corresponds to the value Q = 159 Kj/mole [42,43] can be found from Fig.4 (line 1), Viz., Do ≈ 10 cm^2/S.

3.2 The Known Interpretations of the Anomalies

It is expedient to consider the know interpretations of the anomalous diffusion characteristics as presented by different investigators.

3.2.1 On Anomaly High

Many authors [19,17,6,2] thought that the anomalous high experimental values of D_o^* and Q^* , of transition impurities (Fe, Cr, Mn, Zr, Co) diffusion in Al, characterized true volume diffusion proceeding by means of vacancy mechanism. The authors conclusion was based on the satisfactory agreement of the theoretical and experimental values of ΔQ despite numerous assumptions inherent in the calculations. According to the authors the model used, half-vacancy electrostatic model, in calculating ΔQ is rather crude. Moreover, they have sighted that there is no satisfactory explanation of the anomalous high values.

The diffusion activation entropy can be estimated, for example for Fe in Al , using the experimental data [6,19] of D_o^* and Ds in the following manner:

The experimental frequency factor ratio is

$$\frac{D_o^*}{Do_s} = \frac{f}{f_s} \times \frac{x_2'}{x_o'} \exp\left(\frac{\Delta S - \Delta S_o}{R}\right) \exp\left(\frac{-C}{RT}\right), \qquad (3.1)$$

where

$\Delta S = S_2 + S_f$ - the activation entropy of impurity diffusion;

$\Delta S_o = S_o + S_{fo}$ - the activation entropy of self-diffusion;

S_2, S_o - the activation entropies of the vacancy diffusion for the second and Zeroth jump types, respectively;

S_f, S_{fo} - the vacancy formation entropies in the solution and pure solvent, respectively;

$$\nu_2' = \nu_2 \exp(-S_2/R), \quad \nu_o' = \nu_o \exp(-S_o/R). \quad (3.2)$$

For Fe in Aℓ the value of H_2 is large and positive (Table 5); hence $\omega_2 << u$, $c \simeq 0$, $f \simeq 1$, $f/f_s \simeq 1{,}3$.

Taking $\nu_2'/\nu_o \simeq 1$ [28]; $D_{os} = 0{,}1\ cm^2/S$ [6] and

$D_o^* = 6x10^3 cm^2/S$ [19] (Table 2); substitution in Eq.(3.1) gives,

$$\frac{D_o^*}{D_{o_s}} \exp\left(\frac{\Delta S - \Delta S_o}{R}\right) \simeq 6x10^4$$

where

$$\Delta S - \Delta S_o \simeq 11R ,$$

According to the estimations of [54,55] $\Delta S_o \simeq R$. Hence $\Delta S = 12R$, that is close to the entropy change of sublimation (evaporation) of Aℓ . It is evident that such entropy change can not occur during atomic diffusion (Fe) in the crystal (Aℓ) by vacancy mechanism. Therefore, such interpretation [19,17,6,2] of the anomalous high values of the diffusion characteristics (D_o^*, Q^*) thought to be erroneous.

3.2.2 On Anomaly Low

The authors [20,23] regarded the anomalous low values ($D_{o\ell}$ and Q_ℓ) they have obtained, for the diffusion of Fe, Co, Ni.and Cr in the near-surface strata (~1-10μm) in Aℓ , to be characterized by preferential diffusion along dislocations (with segregational dislocation density $\rho_d \approx 10^8 cm^{-2}$), and can be described by the help of Hart equation [56]:

$$D_{eff} = D_d \eta_d + D(1-\eta_d), \qquad (3,3)$$

where

D_d - the true diffusion coefficient of the impurity along dislocations;

η_d - the fraction of all atoms (the matrix and impurity) in the dislocation regions, out of the total number of atoms in the sample or crystal;

D - the true diffusion coefficient of the impurity in the volume (lattice) of the crystal;

D_{eff} the effective volumetric diffusion coefficient of the impurity (experimental value).

Due to the low solubility of the impurities (Fe,Co,Ni,Cr) in Aℓ , the authors [20,23] thought that the volume diffusion can be disregarded, therefore,

$$D_{eff} \approx D \approx D_d \eta_d , \qquad (3,4)$$

where

$$\eta_d \approx \rho_d \, b^2 \approx 10^{-7} , \quad \rho_d \approx 10^8 \ cm^{-2}$$

b - the Burger's vector in Aℓ, $b^2 \approx 10^{-15} cm^2$ [52].

This approach was reproved by Bulluffi [57]. He showed that it was impossible to neglect the volume diffusion, the second term on the right in Eq.(3.3). At high temperatures, where D_ℓ [20] is taken, the value of the volume diffusion coefficient, $D(1-\eta_d) \approx D$, indeed exceeds by several orders the value of D_ℓ [20] if D is taken to be close to the self-diffusion coefficient of Aℓ , D_s [4,5,6], or if it is taken to be equal to D^* [8,19].

It is vital to consider the possibility of using a more exact equation; i.e., the Hart-Mortlock equation [58]:

$$D_{eff} = \alpha \rho_d b^2 k_d D_d + D , \qquad (3.5)$$

where

α - the number of all the atoms (impurity and matrix) in the cross section of the impurity segregated regions along dislocations,

$K_d = \frac{C_d}{C}$ - the distribution coefficient of the impurity atoms between the segregation regions along dislocations and the crystal volume,

C_d - the local concentration of the impurity atoms in the segregation regions along dislocations,

C - the volume concentration of the impurity in the crystal.

In Eq.(3.5), if $D \gg \alpha b^2 \rho_d k_d D_d$ the effective diffusion coefficient is nearly equal to the true volume diffusion coefficient, $D_{eff} \approx D$; i.e., the diffusion proceeds with normal characteristics (Do,Q). On the contrary,

$D << \alpha b^2 \rho_d \, k_d \, D_d$, $D_{eff} \approx \alpha b^2 \rho_d \, k_d \, D_d$; i.e., the diffusion proceeds along the near dislocation segregation regions with a higher rate than the volume diffusion.

From both Eqs. (3.3) and (3.5) it follows that D_{eff} can not be smaller than D as it is in the interpretation of the authors of the work [20].

Later on Murarke, Anand and Agarwala [23] considered that the anomalous low values of $D_{o\ell}$, Q_ℓ and D_ℓ of transition impurities (V, Cr, Pd, Fe, Co, Ni) in Aℓ characterized the true volume diffusion.

Mortlock [59], however, analysed some experimental data ([20], and others) and came to the conclusion that the values of $D_{o\ell}$, Q_ℓ and D_ℓ obtained characterized neither the true volume diffusion nor diffusion along dislocations. He, thus, suggested that further investigation would be necessary for proper interpretation.

3.3 The Experimental Methods and Conditions of Obtaining The Diffusion Characteristics

Some authors [6,8,19] argued that the anomalous low values were caused by systematic errors because of not taking into account the delay action of the surface oxide film - $A\ell O_3$ - which, according to their opinion, is exhibited highly if the electrolytic [20] or chemical [24,20] methods of isotope depositing is used. Therefore, it is advantageous to examine the experimental methods and conditions of getting the anomalous and normal diffusion characteristics.

3.3.1 Surface Oxide Film and Near-Surface Effect

In the investigations [20,23-26] in which the anomalous low values ($D_{o\ell}$, Q_ℓ) were found, the authors used the electrolytic [20] or chemical [24,20] methods of isotope depositing without providing conditions of minimizing the surface oxide film. Under these conditions the penetration profile for the diffusion of a transition impurity in Aℓ , produced during diffusion annealing at high temperatures with several hours duration, did not exceed 1-10μm from the sample surface.

On the other hand, in the investigations [6,8,9,17-19] where the anomalous low values ($D\mathring{\delta}$, Q^*) were obtained, the authors used special methods of depositing the isotope thereby by providing conditions of reducing or removing the surface oxide film. Under these conditions the concentration profile of a transition impurity, created during diffusion annealing at high temperatures with the same time duration, reached about a hundred micro-meters depth from the sample surface. Nevertheless, there was the so-called near-surface effect which resulted in a sharper decline of the isotope concentration in the near-surface region (about 1-10μm depth) than followed by the extrapolation of the concentration profile in the remote regions from the sample surface. In other words, the near-surface effect manifests abnormally high delaying action, in the near-surface zone of the sample, on the impurity which is diffusing into the bulk.

Alexander and Slifkin [8] noted that when near-surface effect is manifested the concentration profile could be described by two Gaussian curves. One of which, localized in the near-surface zone, corresponds to the anomalous low diffusion characteristics ($D_0\ell$, $Q\ell$, $D\ell$) which was neglected frequently by many investigators in finding the diffusion characteristics. The second curve, localized in far-distant regions of the smaple, as usual corresponds to anomalous high diffusion characteristics (D_0^*, Q^*, D^*) or to the normal (Do, Q, D).

Alexander and Slifkin also suggested [8] that if the near-surface effect was caused by delaying action of the surface oxide film then the concentration profile should be described by one Gaussian curve only. Moreover, there should be rather higher local isotope concentration near the sample surface.

3.3.2 The Physical Interpretation of The Near-Surface Effect

The experimental results [60] of Tiwari and Sharma are notable for physical interpretation of the near-surface effect. They investigated diffusion of Fe in Aℓ using electrolyting method of isotope depositing, exactly as in the case of Agrawala et al [20]. In their work, diffusion of Fe isotope was investigated in polycrystalline Aℓ specimens which were prediffusing-annealed at 893K for periods varying from 2 to 3 hours to about 15 days. The following diffusion annealing, for instance at 823K for a period of

$5.2x10^5$S, caused the concentration profile formation within a depth less than or equal to 7μm (Fig.5). The profile corresponded to the anomalous low characteristics in accordance to the data of Agrawala et al. The prediffusion-annealed samples contained lower dislocation density, according to their measurement by about one order, Similar diffusion annealing caused the concentration profile formation within a rather larger depth, about 20μm (Fig.5). This profile corresponded to the anomalous high diffusion characteristics in accordance to that of anomalous high reports [8,19]. The methods of isotope depositing used in the works [8,19] of Alexander and Slifkin, and Hood were different from that of Tiwari and Sharma. But in the near-surface region, about 7μm, there was sharp decreasing of the isotope concentration as compared to far distant regions (Fig,5). In other words, the near-surface effect was exhibited.

Based on the fact found, increasing of the diffusion coefficient (approximately by two orders) due to decrease in dislocation density (approximately by one order), Tiwari and Sharma [60] concluded that the slow diffusion of Fe in Aℓ, in the near-surface zone (of Aℓ), proceeded with anomalous low characteristics ($D_{o\ell}$, Q_ℓ) due to the capture of the diffusing atoms by dislocations in the near-surface zone. Thus, they suggested that anomalous results cannot be attributed entirely to the presence of an oxide layer.

Furthermore, Tiwari and Sharma showed that the assumption [19,8,6] the anomalous low values of the diffusion characteristics ($D_0\ell$, $Q\ell$, $D\ell$) were due to systematic errors, in particular the delaying action of the surface oxide film, was groundless.

The results obtained lead to the conclusion that the near-surface effect and the anomalous diffusion characteristics are caused by high dislocation density in the near-surface layers of the metal. The high dislocation density in the near-surface zone of the metal can be caused by relaxation of the elastic tension (strain stress) near the interphase boundary, "metal-oxide" or "metal-intermetallic compound" [52], or by intense change in the concentration gradient of the impurity in the near-surface zone [52], etc.

Review of the experimental data lead to the auumption that diffusion proceeds with anomalous low characteristics ($D_0\ell$, $Q\ell$, $D\ell$) if the dislocation density is rather high. Such a high dislocation density can exist in the near-surface layer of the metal, especially after electrolytic or chemical isotope depositing. In far distant layers, where the dislocation density is not so high, diffusion can proceed with anomalous high characteristics (D_0^*, Q^*, D^*), which is faster than diffusion with anomalous low characteristics but obviously slower than normal diffusion (D_0, Q, D). Evidently, diffusion proceeds with normal characteristics if the dislocation influence is neglegible.

Diffusion of solute atoms (Fe) in particles of the second phase (Fe $A\ell_3$) in Aℓ matrix was studied [42,43] under conditions when the mean distance between neighbouring particles was less than or equal to the mean distance between dislocations (electron microscope data). Clearly, it is under these condtions that dislocations can not significantly influence the impurity diffusion. According to the data considered above [44] it is possible to assume that ordinary dislocation density (10^7-10^8 cm^{-2}) does not influence the diffusion of Fe in very dilute Aℓ solutions (containing about 10^{-7} atomic fraction of Fe) when the main part of Fe is in the solid solution (Mossbauer data). In view of the data [5] of diffusion of Mn in Aℓ (conditioned to plastic deformation of the sample during diffusion annealing), it can be assumed that moving dislocations do not influence the impurity diffusion.

Therefore, it is worthy to assume that diffusion anomalies can be caused by the influence of some form of segregation phases on motionless dislocation. In order to explain the experimental data considered so far it is essential to develope some sort of physical model based on the influence of dislocations decorated by segregation phases upon the impurity diffusion.

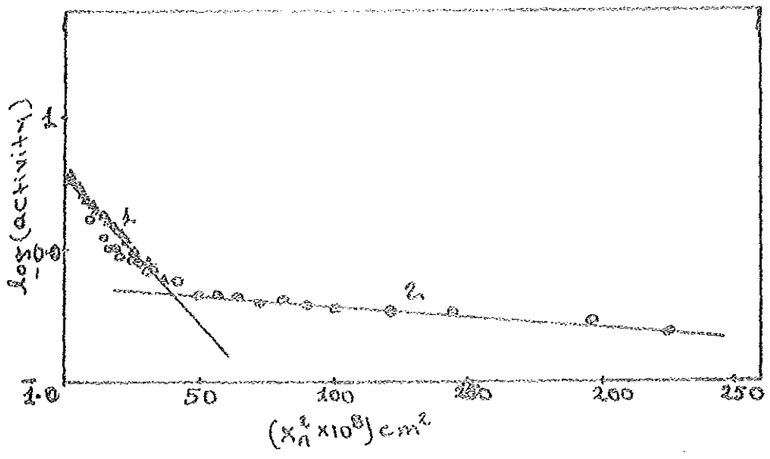

Fig 5. The concentration profiles for diffusion of Fe^{59} in Al polycrystals(data of Tiwari and Sharma [60])

1. Diffusion annealed at 823 K for 5.23×10^5sec, $D_g = 1.10\times10^{-13}\,cm^2/s$ (the samples were preannealed for 7hrs at 593K)
2. Diffusion annealed at 853K for 1.95×10^4sec $D^M = 2.50\times10^{-11}\,cm^2/sec$ (the samples were pre-annealed for 15 days at 593k).

CHAPTER 4

INTERPRETATION AND DESCRIPTION OF THE DIFFUSION ANOMALIES

No single one of the interpretations discussed so far (Chapter 2 and 3) can account satisfactorly for the transition impurity diffusion anomalies. A synthesizing model is still needed to include the effect of dislocations decorated by segregation phases. Furthermore, the model needs to be of such a form that it can be used to predict diffusion behaviour under given conditions and be useful for proper interpretation of the experimental data.

4.1 The Effective Diffusion Coefficient

In relation to the preceding chapters it is valuable to consider the corresponding diffusion equation in order to derive expression for the effective diffusion coefficient of an impurity diffusing in a crystal with dislocation lines decorated by some form of segregation phases.

4.1.1 The Diffusion Equation

Consider a one-dimensional diffusion of an impurity along two neighbouring regions having different cross-sectional areas (S_1, S_2) and diffusion coefficients (D_1, D_2).

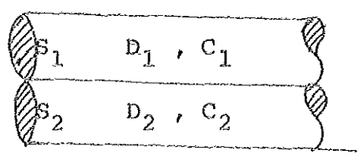

A diffusion equation of the regions can be derived in two limiting ways:

1. Impenetrable Partition. The boundary between the two regions is assumed to be impenetrable to impurities. If diffusion is one-dimensional i.e., if there is a gradient of concentration only along the x-axis the flux densities (J_1, J_2) of the two regions are given by Eq.1.1b, Viz.

$$J_1 = - D_1 \frac{\partial C_1(x,t)}{\partial x}$$

$$J_2 = - D_2 \frac{\partial C_2(x,t)}{\partial x}$$

where C_1 and C_2 are the concentrations of the impurity in the two regions, which depend on both time and distance. The total diffusion flux of the impurity atoms is then the sum of the fluxes due to the two regions, i.e.,

$$SJ = - D_1 S_1 \frac{\partial C_1}{\partial x} - D_2 S_2 \frac{\partial C_2}{\partial x} ,$$

where $S = S_1 + S_2$ is the total area. The total flux density can be written as

$$J = - D_1 \eta_1 \frac{\partial C_1}{\partial x} - D_2 \eta_2 \frac{\partial C_2}{\partial x} ,$$

where,

$$\eta_1 = \frac{S_1}{S_1 + S_2} , \quad \eta_2 = \frac{S_2}{S_1 + S_2}$$

For a given constant temperature ($T_1=T_2=T=$constant) and dilute solution (where $D_1, D_2 \neq f(x,t)$), the employment of the equation of continuity gives,

$$D_1\eta_1 \frac{\partial^2 C_1}{\partial x^2} + D_2\eta_2 \frac{\partial^2 C_2}{\partial x} = \eta_1 \frac{\partial C_1}{\partial t} + \eta_2 \frac{\partial C_2}{\partial t}$$

where,

$$C = \frac{C_1S_1 + C_2S_2}{S_1 + S_2} = C_1\eta_1 + C_2\eta_2 \ ,$$

the total concentration, is used. If $S_1 >> S_2$ then

$\eta_1 \simeq 1$ and $\eta_2 \simeq S_2/S_1$.

Thus,

$$D_1S_1 \frac{\partial^2 C_1}{\partial x} + D_2S_2 \frac{\partial^2 C_2}{\partial x} = S_1 \frac{\partial C_1}{\partial t} + S_2 \frac{\partial C_2}{\partial t} \ , \qquad (4.1)$$

Eq.4.1 is the desired diffusion equation.

2. Local Equilibrium Distribution. In this hypothesis the boundary between the two regions is penetrable to impurities and the impurity atoms streaming from one region to the other are equilibrious.

   The workability of using this hypothesis can be verified from the concept of relaxation time. The local equilibrium approximation between the near dislocation regions and the matrix solution might be used if the inequality [61]

$$Dt\,\rho_1 >> 1 \ , \qquad (4.2)$$

holds, where t is the diffusion time, ρ is the dislocation density and D diffusion coefficient. The rms distance ($\bar{x}^2$) covered by a diffusing atom varies as

$$\bar{x}^2 = Dt \quad . \tag{4.3}$$

Using these two equation

$$t_{ann} \simeq \frac{\bar{x}^2}{D} >> \frac{1}{D\rho_{\perp}} \simeq \tau \quad ,$$

where t_{ann} is the annealing time and τ time of attaining local equilibrium. For Fe in Al using $D_o \simeq 10 cm^2/5$, $Q \simeq 159$ KJ/mole and $\rho_{\perp} = 10^9 - 10^{10}$ $cm^2/5$ [62] ; hence $\tau \simeq 0,15$. Comparing τ with the usual annealing time, 1-10 hrs., indeed $t_{ann} >> \tau$. Thus, the annealing time being greater than time of attaining local equilibrium it is possible to use local equilibrium approximation.

The impurity exchange between the two region being in balance, there is no need to consider the perpendicular fluxes. The fluxes can be thought to be quasi-independent. Hence, equation (4.1) can be obtained quite similarly.

4.1.2 The Approximations of the Effective Diffusion Coefficient

In local equilibrium approximation between the two regions the simplest distribution law, which is characterized by

a linear concentration dependence, can be considered;

$$\frac{C_1}{C_2} = K = \text{constant, if } T = \text{constant,} \qquad (4.4)$$

where K is the corresponding distribution constant of the impurity between the two regions. K is not function of the concentrations ($K \neq f(C_1, C_2)$) instead it is function of temperature ($K = f(T)$).

If Eq.(4.4) is substituted in Eq.(4.1)

$$\left(\frac{D_1 + D_2 \eta K}{1 + \eta K}\right) \frac{\partial^2 C_{1(2)}}{\partial x^2} = \frac{\partial C_{1(2)}}{\partial x} \quad , \qquad (4.5)$$

here $\rho = S_2/S_1$ and the term in the braket is the effective diffusion coefficient. The region occupied by dislocations decorated by segregation phases is so small compared to the lattice undisturbed by dislocations. Subsequently the effective diffusion coefficient of an impurity, in a crystal with dislocations decorated by segregation phases, can be approximated as:

$$D_{eff} = \frac{D + D_\perp \eta_\perp K_\perp}{1 + \eta_\perp K_\perp} \quad , \qquad (4.6)$$

where D is the matrix diffusion coefficient of the impurity in the undesturbed lattice,

$$D = D_o \exp(-Q/RT) \quad ; \qquad (4.7)$$

$D_\perp$ is the diffusion coefficient of the impurity in the dislocation pipe (in the segregation phase regions along dislocations),

$$D_\perp = D_{O\perp} \exp(- Q /RT) \; ; \qquad (4.8)$$

$\eta_\perp$ is the fraction of all atoms in the segregation phase regions near dislocations,

$$\eta_\perp = \alpha b^2 \rho_\perp \; , \qquad (4.9)$$

b is the Burgers vector in the crystal, α is the total number of atoms in the cross-sectional area of the segregation phase regions near dislocations and $\rho_\perp$ is the dislocation density. $\eta_\perp << 1$ (since it is of the total number of atoms in a crystal). $K_\perp$ is the equilibrium constant of the process of impurity distribution between the matrix solution and the segregation phase regions near dislocations,

$$K_\perp = \exp(-\Delta S_\perp/R) \exp(\Delta H_\perp/RT) \; , \qquad (4.10)$$

$\Delta S_\perp$, $\Delta H_\perp$ are the entropy and enthalpy changes of the system when one mole of the impurity atoms passes from the segregation phase regions near dislocations to the matrix.

Case-1. If $\eta_\perp K_\perp << 1$ (i.e., most of the impurity atoms are localized in the matrix solution) then expression (4.6) is reduced to that of Hart-Mortlock expression, which cannot explain the diffusion anomalies considered in the preceding chapter.

Case-2. If $\eta_\perp K_\perp \gg 1$ (i.e., the most part of the impurity atoms are localized in the segregation phase regions near dislocations) then the effective diffusion coefficient can be expressed as

$$D_{eff} \approx D/\eta_\perp K_\perp + D_\perp \quad , \tag{4.11}$$

where it follows that $D_{eff} < D$ if $D_\perp < D$.

Eq.(4.11) in turn reduces to two limiting cases:

a) In case $D_\perp \gg D/K_\perp \eta_\perp$, then,

$$D_{eff} \approx D_\perp = D_{O\perp} \exp(-Q_\perp/RT) \quad , \tag{4.12}$$

i.e., the prevaling diffusion is that along the segregation phase regions near dislocations which is characterized by $D_{O\perp}$ and $Q_\perp$.

b) In case $D_\perp \ll D/K_\perp \eta_\perp$, then,

$$D_{eff} = D^* = \frac{D}{1+\alpha b^2 \rho_\perp K_\perp} \tag{4.13}$$

In this case the prevaling process is retarded volume diffusion of the impurity atoms accompanied by in an out pumping of the impurity atoms to the near dislocation regions. The prevaling process proceeds with anomalously high characteristics:

$$D_O^* = \frac{D_O}{\alpha b^2 \rho_\perp} \exp\left(\frac{\Delta S_\perp}{R}\right) \quad , \tag{4.14}$$

$$Q^* = Q + \Delta H_\perp \quad . \tag{4.15}$$

4.1.3 The Critical Temperature

As the diffusion annealing temperature of a crystal containing sufficiently high dislocation density is raised, transition can occur from one diffusion mechanism ($D_{O\perp}$, $Q_\perp$) to another (D_O^*, Q^*). Since Q^* is several times larger than $Q_\perp$ such transition can occur in a narrow temperature range. In light of this it is possible to consider a critical temperature, T_c, whose dependence on the dislocation density ρ is determined by equating the two right hand terms in Eq.(4.11) at this temperature,

$$\frac{1}{T_c} \simeq A - B \log \rho_\perp \quad , \tag{4.16}$$

where,

$$A = \frac{R}{Q^* - Q_\perp} \frac{\Delta S_\perp}{R} + \log \left(\frac{D_O}{D_{O\perp} \alpha b^2}\right) \quad , \tag{4.17}$$

$$B = \frac{R}{Q^* - Q_\perp} \tag{4.18}$$

Obviously, at $T > T_c$ the diffusion process with characteristics Q^* and D_O^* will occur (at a sufficiently high $\rho_\perp$ and $T < T_{m.p.}$) At $T < T_c$ the diffusion with characteristics D_O and Q proceeds in the crystal with the given dislocation density, $\rho_\perp$. This concept gives satisfactory description (qualitative as well as quantitative) of the diffusion anomalies.

4.2 Interpretation of the Experimental Data

The anomaleus high and low experimental data obtained by different investigators are treated by the description developed in section 4.1.

4.2.1 The Anomalous High Treatment

For instance, the diffusion coefficient D^* experimental values [8,19,60] of Fe in Aℓ can be described using Eq.(4.6) in case where $D >> D_\perp \eta_\perp K_\perp$ and $\eta_\perp K_\perp >> 1$. In this case Eq.(4.6) can be represented by Eq.(4.13) or as follows

$$\log\left(\frac{D}{D^*} - 1\right) = \log(\alpha b^2 \rho_\perp) - \frac{\Delta S_\perp}{R} + \frac{\Delta H_\perp}{RT} \,. \qquad (4.13^*)$$

using the experimental data [8,19,60] of the values of D^* at high temperatures and assuming $D_o \simeq 10 cm^2/S$ and $Q = 163$ KJ/mole for "normal" diffusion of Fe in Aℓ (Chapter 3) it is possible to draw $\log(D/D^* - 1)$ versus $10^3/T$ in order to find the values of $\Delta H_\perp$ and $\alpha b^2 \rho_\perp \exp(-\Delta S_\perp/R)$; Fig.6. Such treatment of the data of D^* and D gives

$$\Delta H_\perp = 86.2 \pm 9.2 \text{ KJ/mole}$$

and

$$\alpha b^2 \rho_\perp \exp(-\Delta S_\perp/R) = (2.2^{+5.6}_{-2.8}) \times 10^{-5}$$

The value of $\Delta H_\perp$ (from Fig.6) is close to enthalpy of dissolution of the intermetallic compound $FeAl_3$ in Aℓ

lattice (ΔH_{FeAl_3} = 81 ± 3 KJ/mole [63]. This leads to the hypothesis that the structure of the near dislocation regions is close to the structure of the corresponding intermetallic compounds. Taking $\rho_\perp = 10^7$-$10^8 cm^{-2}$ [52,64] and $b^2 = 10^{-15} cm^2$ [52], then $\alpha \exp(-\Delta S_\perp/R) \approx 2x(10^2$-$10^3)$. If $\Delta S = 0$ (the usual approximation then $\alpha \approx 10^2$-10^3 which corresponds to a cross-sectional diameter, the segregation phase regions near dislocations, of about 3-10nm.

Anomalous high characteristic values, diffusion of Mn,Cr, Zr and Co in Aℓ (Table 2), can be described using Eqs. (4.14) and (4.15) if D_o 0.2 - 1 $cm^2/5$, Q = 120-160 $\frac{KJ}{mole}$ and $\rho_\perp = 10^8 cm^{-2}$ are assumed. The rest of the anomalous high characteristic values (Table 2) can be described similarly.

4.2.2 The Anomalous Low Treatment

The anomalously low values of the diffusion coefficient ($D_\perp$) of Fe in the near-surface zone (~1μm) of Aℓat high temperatures (obtained in [23] can be described by Eqs. (4.6) and (4.11) if $\eta_\perp K_\perp >> 1$ and $D << \eta_\perp K_\perp D_\perp$ which have given Eq.(4.12).

Using Eqs.(4.16), (4.17) and (4.18) and the values of $\Delta H_\perp$ and $\alpha \exp(-\Delta S_\perp/R)$ determined above, it is possible to estimate ρ in the near-surface zone (~1μm) of Aℓ polycrystals [23] if $T_c \approx 903K$ is assumed (since in [23] the

the anomalous low values (D_{OL}, $\rho_\perp$, $D_\perp$) of Fe in Aℓ were obtained till 903K). Eq.(6.16) can be transformed to a more convenient form:

$$\rho_\perp \approx \frac{D - D_\perp}{D_\parallel \alpha\, b^2 K_\perp} \approx \frac{D}{D_\parallel \alpha\, b^2 K_\perp} \qquad (4.19)$$

If $D_\perp$ (at 903K) $\approx 1.8\times10^{-12}$ cm^2/s [23] , $D(a+903K) \approx$ 10 cm^2/s $\exp(-163000/8.3\times903) \approx 3.8\times10^{-9}$ cm^2/s and $\alpha K_\perp$ (at 903K) $\approx 1.3\times(10^8-10^7)$ (from Fig.6) are substituted in Eq.(4.19), $\rho_\perp \approx 1\times(10^{10}-10^{11})$ cm^{-2} can be found. Such a high dislocation density in the near-surface zone of Aℓ could be formed, as mentioned in section 3.3, due to relaxation of the elastic stress near interphase boundary and so on [32].

4.2.3 Characteristics of the Segregation Phase Regions Summarized

Thus, the diffusion anomalies data treatment in the frame-work of the developed model gives the following characteristics of the segregation phase regions near dislocations in dilute solutions of transition metals (Fe) in Aℓ:

i) The diameter of the cross-section of the regions is about several nano-meter; so these regions have macroscopic size only in the direction of the dislocation lines.

ii) The effective distribution law of impurity atoms between the near-dislocation regions and the matrix solution might be of a linear character within a certain concentration range. The range in enthalpy, characterizing the "effective energy of binding" between impurity atoms and the near-dislocation regions, turned out to be close to enthalpy of dissolution for the corresponding intermetallic compound (in the metallic matrix).

iii) Transition impurities diffusion in the near dislocation regions proceeds with anomalous low characteristics ($D_{O\perp}$, $Q_\perp$, $D_\perp$) compared to the metallic matrix ($D_{O\perp} << D_O$, $Q_\perp < Q$, $D_\perp << D$).

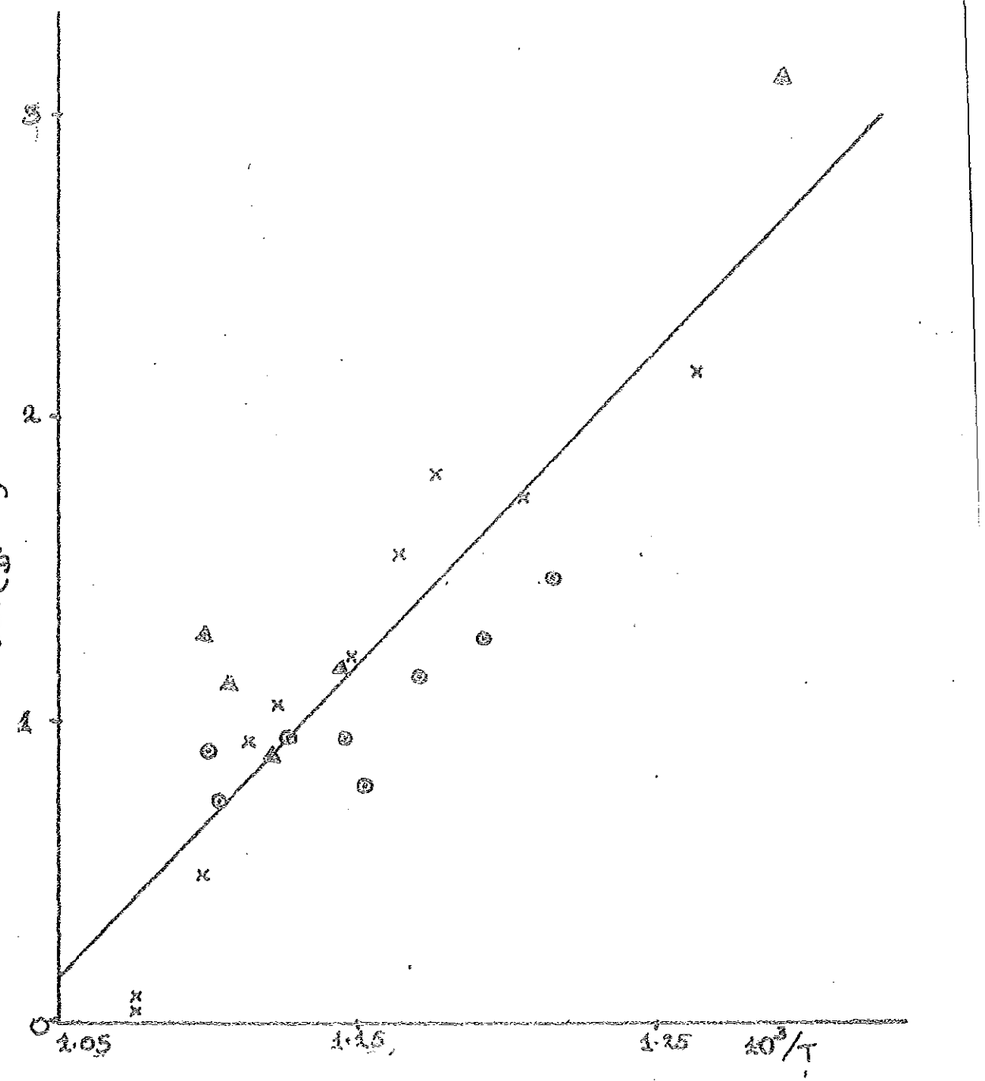

Fig 6. Graphs for estimating the effective binding energy ΔH_{Bi} of Fe atoms in the near dislocation region in Al and the value of the pre-experimental factor of the distribution coefficient $\omega^2 S_i \exp(-\Delta S_{Bi}/R)$ using the experimental data [19] (11 "point" x) 8 (8points ◎) and 60 (5 "points" △)

CHAPTER 5

SUGREGATION OF SUBSTITUTIONAL IMPURITIES IN NEAR DISLOCATION REGIONS

As it is aforementioned, the notion about "impurity atmosphers" or impurity clouds" near dislocations were introduced for the first time by Cottrell [65] and Nabarro [66] in papers concerning the yield and ageing behaviour of low-carbon steels. The key physical concept introduced in these papers is that an interaction between dislocations and solute atoms causes the solute atoms to migrate to, and surround dislocations with a cloud or atmosphere.

In certain alloy systems distinct phases occur where the constituent atoms are in fixed integral ratios, e.g., $FeAl_3$. Such an intermetallic compound is held together by metallic bonds and may form a very complicated crystal structure. In particular, transition impurity atoms have very low solid solubility in the matrix (Al) which leads to segregation phase (intermetallic compound) formation when the impurity concentration in the matrix exceeds the limiting solubility.

It is expedient to compare the characteristics of the segregation phase obtained in section 4.2 with the known theoretical and experimental data of substitutional impurity segregation (Cottrel cloud) and segregation phases (Intermetallic compounds) in the near dislocation regions in f.c.c. metals.

5.1 The Cottrell Cloud

The amount of energy must be expended in order to dissociate the solute atom from the dislocation is estimated from thermodynamics point of view. Furthermore, it is shown that this type of segregation model is inadequate to explain the diffusion anomalies.

5.1.1 The Various Expressions for the Distribution of Solute Atoms Relative to a Straight Dislocation

Consider an ideal binary solid solution containing a single, straight dislocation of arbitrary Burgers vector.

The local concentration (in atomic fraction) of an impurity atoms at position r from the dislocation axis, from thermodynamic point of view, for dilute solution, is approximated [67].

$$C(r) = \{\exp[(-\Delta G(r)-\varepsilon)/RT] + 1\}^{-1} , \qquad (5.1)$$

where R is gas constant; T absolute temperature; ε is the maximum strain amplitude, solute atom "Fermi" energy, which is given by

$$\varepsilon = RT \log [C_\infty /(1-C_\infty)] . \qquad (5.2)$$

The solute atom-dislocation interaction is characterized by an interaction free energy $\Delta G(r)$ which is defined as the change that occurs in the Gibbs free energy of the solid when a solute atom migrates from a position vector r, originating at and perpendicular to the axis of a straight

dislocation of arbitrary Burgers vector, to position "infinitely" removed from the dislocation. The quantity $\Delta G(r)$ and $C(r)$) is a function of the solute atom's position relative to the dislocation, and varies in magnitude from zero when the solute is infinitely removed ($r = \infty$), to a value of $G(0) = G_B$ at the position of maximum interaction at the dislocation axis (Fig.7). The latter quantity is defined as the binding free energy of the solute atom to the dislocation. The binding free energy, in turn, is related to the binding enthalpy H_B and the binding entropy S_B by the expression,

$$G_B = H_B - TS_B \quad , \tag{5.3}$$

When $(-\Delta G(r) - \varepsilon) >> RT$, equation (5.1) reduces to

$$C(r) \approx \exp[(\Delta G(r) + \varepsilon)/RT] \quad . \tag{5.4}$$

Equations (5.1) and (5.4) prescribe the distribution of solute atoms relative to a straight dislocation for the ideal approximation.

The solute concentration far removed from the dislocation, C_∞, has to be less than the average bulk solute concentration, $\bar{C}$, in the interval $0 < T < \infty$; Viz., $0 < C_\infty < \bar{C}$ (Fig.7).

If r and θ represent the position of an impurity atom relative to the dislocation axis and the angle between the position vector (r) and the dislocation slip plane in

cylinderical coordinates then the density of sites (per unit length of dislocation) between r and r + dr and θ and θ + dθ is $g(r, \theta)$ (if $\Delta G(r)$ is evaluated on a continuum basis). Thus, $g(r, \theta)dr\, d\theta$ is given by the expression [67].

$$g(r, \theta)\, dr\, d\theta = \frac{1}{V} r\,d\, r\,d\theta \,, \qquad (5.5)$$

where V is the atomic volume. If equation (5.5) is integrated over all θ (0 to 2π) and r (from zero to some upper limit R_o ; i.e., one-half the mean distance between dislocations), the total number of atomic sites per unit length of dislocation (N) is obtained.

The total number of solute atoms is expressed, using Eqs. (5.1), (5.2) and (5.5), as follows:

$$\bar{C}N = \frac{1}{V} \int_0^R \int_0^{2\pi} \frac{r\,d\, r\,d\theta}{\exp[(-\Delta G(r,\theta) - \varepsilon)/RT] + 1} \,. \qquad (5.6)$$

Before the integrals can be evaluated, an analytic form for $\Delta G(r,)$ must be inserted into Eq.(5.6), i.e.,

$$\Delta G(r,\theta) = \frac{G_B\, b\, \sin\theta}{r} \,, \qquad (5.7)$$

where b is the magnitude of the Burgers vector of the interacting dislocation. Unfortunately Eq.(5.6) can not be integrated in closed form with this expression for $\Delta G(r,\theta)$. However, if $\Delta G(R_o,\theta) << RT$, then the equation reduces to the simple relation

$$\bar{C} = C_\infty/(1 - C_\infty) \,. \qquad (5.8)$$

Obviously, this relation holds provided it is possible to neglect the decrease in volume impurity concentration due to segregation regions formation near dislocations. In particular, for sufficiently dilute solution, in which the volume concentration decrease is negligible, it is possible to assume that

$$\varepsilon \approx RT\ell n\bar{C} \qquad (5.9)$$

Fig.8 schematically depicts the distribution function $C(r,\theta)$, the density of sites $g(r,\theta)$, and their product, the density of occupied (by solute) sites for an arbitrary θ. The cylindrical cut-off radius r_c is necessary, since most determinations of $\Delta G(r)$ are not valied for positions less than a few atomic diameters from the dislocation axis.

It is also is of some importance to determine the temperature T_c at which the solute atom atmosphere condenses into a compact configuration. Arbitrarily, condensiation is defined to occur when $C(0)$, the atom fraction of solute at the dislocation core, equals 0,5. Since the core concentration is of pivotel interest, and since from Eq.(5,1) $C(0) = 0,5$ only when $\varepsilon = G_B$, Eqs. (5,3), (5,2) and (5,8) yield:

$$T_c = H_B/(S_B + R\ell n\bar{C}) \quad , \qquad (5,10)$$

S_B and $\Delta S(r)$ are usually assumed to be equal to zero for ideal solution. Rude consideration of vibrational entropy S_B (in pinned elastic string model of dislocation, near

impurity atoms) gives twofold effective binding energy [68,69] , Eq.(5.1), for r = 0, can then be represented as:

$$C_o = \{\exp[-2(H_B + \varepsilon)/RT] + 1\}^{-1} \quad . \qquad (5.11)$$

For non-ideal solution of the impurity atoms in the near dislocation regions the concentration can be found in the framework of "regular" solution theory in quasi chemical approach, where the chemical contribution of the binding entalpy $H(r)$ and binding entropy $\Delta S(r)$ are assumed to be equal to zero. For such a case the following expression, for $C_\infty \ll 1$, is associated [67].

$$C(r) = \{\exp[(-\Delta H(r) + C(r) N_A Z\phi - \varepsilon)/RT] + 1\}^{-1} \quad , \qquad (5.12)$$

where Z is the coordination number; N_A Avogadro number; ϕ local order parameter

$$\phi = 2\varepsilon_{AB} - \varepsilon_{AA} - \varepsilon_{BB} \quad , \qquad (5.13)$$

ε_{AA}, ε_{BB}, ε_{AB} - are energies of pair interaction of matrix atoms (A-A), impurity atoms (B-B) and matrix-impurity atoms, respectively; all ε are negative since they take zero value at infinite separation between the atoms.

Eq.(5.12) is transcendental (with respect to C(r)); for this reason extra contribution to the effective binding energy from local ordering interaction enthalpy is usually considered, which is expressed as [70].

$$\Delta H_{(\text{local order})} = - \bar{C}(r) N_A Z\phi \quad , \qquad (5.14)$$

where $\bar{C}(x)$ is the average concentration at a distance x. In finding the total interaction enthalpy this expression should be included.

Since local ordering occurs when $\phi \neq 0$, inspection of Eq.(5.12) shows that solute-dislocation binding is diminished in systems where solute-solute interaction are attractive ($\phi > 0$), and enhanced when interactions are repulsive ($\phi < 0$).

The value of ϕ can be calculated, for example, from the phase diagram of A-B the expression describing the temperature dependence of the limiting solubility of impurity B in matrix A.

For substitutionla impurities in f.c.c. metals $ZN_A\phi/2 \approx 10\text{-}30$ KJ/mole [71], $\bar{C}(x) \approx 0.1$ at $x \approx b$, which yields $\Delta H_{(\text{local order})} \approx 2\text{-}6$ Kj/mole.

For description of impurity atmospheres Eqs.(5.1)-(5.10) are usually used. The entropy factor is often neglected (i.e., $\Delta S(x)$ and S_B are equated to zero for ideal solution).

5.1.2 Contributions to the Interaction Free Energy

A number of contributions to the interaction enthalpy $\Delta H(x)$ should be considered in order to evaluate the total interaction free energy. In finding $\Delta H(x)$ several components caused by elastic, electrostatic and electrochemical interactions of the impurity atoms with dislocations are considered. For

dilute solutions, the contributions are assumed to be mutually independent. The individual contributions are considered as follows.

The Elastic Misfit Interaction. For edge dislocation the main contribution to $H(x)$ is attributed to the elastic interaction which is due to the difference in size of impurity and matrix atoms. Based on isotropic continuum the elastic misfit interaction can be expressed as [67].

$$\Delta H_{(\text{Elastic Misfit, Edge})} = \frac{-4N_A \mu b \eta_a r_o^3 \sin\theta}{r}, \qquad (5.15)$$

$$H_{B(\text{Elastic Misfit, Edge})} = -4N_A \mu \eta_a r_o^3, \text{ (if } r=b), \qquad (5.16)$$

where μ-shear modulus; r_o-atomic radius of the metal-solvent (in unstressed state); b-Burgers vector. The solute dilation η_a due to the impurity atom introduction, commonly termed the size misfit parameter, is defined by the expression:

$$\eta_a = \frac{r' - r_o}{r_o}, \qquad (5.17)$$

where r'-effective impurity atom radius in metal-solvent in stressed state.

The value of η_a can be obtained experimentally, for example, from x-ray measurement of the concentration dependence of the lattice parameter (a), with the aid of the expression [67].

$$\eta_a = \frac{1}{a} \frac{\partial a}{\partial c}, \qquad (5.18)$$

where $(\partial a/\partial \bar{C})$ is the rate of change of alloy lattice parameter with solute composition.

Evaluation of H_B using Eq.(5.16) (assuming $r_c \simeq b$) for some substitutional impurities (Ni, Zn, Ga, Ge, As) in copper gave a value of 10-50 KJ/mole (Table 6). At $r = 3nm$ according to Eq.(5.15) the value of $\Delta H(r)$ decreases approximately by one order (as compared to H_B). For the case of screw dislocations $\Delta H(r)$, due to elastic misfit effect of substituted impurities in f.c.c. metals, is approximately by one order lower than that of edge dislocation.

Eq.(5.15) can be written as [52,67],

$$\Delta H(r)_{(\text{Elastic Misfit,Edge})} = \frac{-\mu b(1+\nu)N_A(V_1-V_o)\sin\theta}{3\pi(1-\nu)r} , \quad (5.19)$$

where $V_1-V_o = 4\pi r_o^2(r_1-r_o)$ - difference of volumes of impurity and matrix atoms (in unstressed state); r_1 - radius of impurity atom (in unstressed state); ν - poisson's ratio.

From Eqs.(5.15) and (5.19) follows that the substitutional impurities which have larger atomic volume than the matrix atoms are segregated in the extended regions near edge dislocations and impurities with lesser volume (including vacancies) are concentrated in compressed regions. Estimation of H_B using (4.19) for Fe atoms in Al gave about 17 KJ/mole (at $r = b$); at $r \simeq 3nm$ the value of $\Delta H(r)$ decreases nearly by one order.

The Elastic Modulus Interaction. A contribution to the interaction enthalpy H(r) arises whenever the impurity and metal-solvent possess dissimilar elastic moduli. This elastic modulus enthalpy, based on linear elastic theory, is found to be [72] :

1. For edge dislocation

$$\Delta H(r)_{(\text{Elastic Modulus, Edge})} = -N_A[\mu b_e^2 r_o^3/6\pi(1-\nu)^2 r^2] \times$$

$$\times \left[\frac{2}{3}\eta_\beta(1+\nu)(1-2\nu)\sin^2\theta + \eta_\mu\cos^2\theta\right] ; \qquad (5.20)$$

2. For screw dislocation

$$\Delta H_{(\text{Elastic Modulus, Screw})} = \frac{N_A \mu b_s^2 r_o^3 \eta_\mu}{6\pi r^2} ; \qquad (5.21)$$

where b_e and b_s - the magnitudes of the edge and screw components of Burgers vector, respectively. Here η_β is bulk modulus inhomogeneity parameter, and is given by

$$\eta_\beta = (\beta'-\beta)\{\beta-[(1+\nu)/3(1-\nu)](\beta-\beta')\}^{-1} , \qquad (5.22)$$

where β' and β are bulk moduli of the inclusion and the matrix, respectively. η_μ is shear modulus inhomogeneity parameter, and is given by

$$\eta_\mu = (\mu'-\mu)\{\mu[(8-10\nu)/15(1-\nu)](\mu-\mu')\}^{-1} , \qquad (5.23)$$

where μ' and μ are shear moduli of the inclusion and matrix, respectively.

By analogy with the misfit parameter η_a (see Eq.(5.18)) it is convenient to define the inhomogeity parameters by the macroscopic expressions:

$$\eta_\beta = (1/\beta)\left(\frac{\partial \beta}{\partial C}\right) \quad ; \tag{5.24}$$

$$\eta_\mu = (1/\mu)\left(\frac{\partial \mu}{\partial C}\right) \quad . \tag{5.25}$$

In constrast to Eq.(5.15), Eq.(5.20) indicates that the modulus interaction could lead to binding; i.e., the elastic modulus enthalpy is greater than zero for all θ. Furthermore, if $\eta_\mu = (8/27)\eta_\beta$, Eq.(5.20) prescribes a symmetrical distribution of solute (for $\nu = 1/3$), in contrast to the antisymmetrical distribution prescribed by Eq.(5.15).

It is important to note that the elastic modulus interaction (Eqs.(5.20), (5.21) is calculated by assuming that $\eta_a = 0$; and , the elastic misfit interaction is calculated by assuming that $\eta_\beta = 0$. When both interactions are finite, the individual interaction enthalpies strictly cannot be added algebrically without including a correction term. However, this term involves the product $\eta_a \eta_\beta$, and is small relative to the uncorrected interaction enthalpies.

The isotropic continuum approximation, in which the elastic property of an isolated impurity atom in the solid solution is considered to be equal to the macroscopic properties of the impurity material, is believed to be a rough approximation by many researchers [67].

Calculation of H_B(Elastic modulus) using Eq.(5.20) ($r_c \approx b$ is assumed) for some substitutional impurities (Ni, Zn, Ga, Ge, As) in Cu is obtained to be 3~7 KJ/mole. At $r \approx 3nm$ the value of the binding enthalpy according to Eq.(5.20) decreases nearly by two orders (in comparison with H_B). The same order of $\Delta H(r)$ is obtained for substitutional impurities in f.c.c. metals,

The Electrical Interaction. The electrical interaction of impurities with edge dislocation is connected with redistribution of the conducting electrons in gradient of hydrostatic pressure near dislocation, which leads to formation of electric dipole [73].

Using the Wigner-Seitz method of calculating electron energies the electrical interaction enthalpy between the impurity and dislocation is obtained to be [73].

$$\Delta H(r)_{(Electric)} = -\frac{4}{15} q\varepsilon_F \delta \ , \qquad (5.26)$$

where q - the ratio of the effective impurity charge to the absolute value of the electron charge; ε_F - the energy of the Fermi surface; δ - dilation.

The binding energy due to electrical interaction has a significant value only for small distances between impurity atoms and dislocation lines ($r \approx b$), since the electric field decreases quickly with distance ($\sim r^{-3}$). The value of

H_B (electrical contribution), of an edge dislocation, can be described as [73].

$$H_{B(Electric)} = 2q\ \varepsilon_F(1-2\nu)/15\pi(1-\nu), \qquad (5.27)$$

Cottrell et al not that for a Z-valent impurity atom in Cu, q is equivalent to 0.075(Z-1), and so for edge dislocation in typical substitutional impurities in Cu the electrical interaction enthalpy is approximately by one order less than elastic misfit enthalpy (size effect).

Calculation of H_B (electrical) using Eq.(5.27) for some impurities (Zn,Ga,Ge,Ag) in Cu gave values in the range 1-7 KJ/mole (Table 6). For screw dislocation the electrical interaction binding energy is very much less than for edge dislocations, and is connected with anharmonic expansion of the lattice [52].

The Chemical Interaction. The chemical interaction free energy G_B which is due to the interaction between stacking faults and impurity atoms, can be described by chemical thermodynamics and is given by [74,67]

$$G_{B(Chemical)} = \frac{-V}{h} N_A \frac{\partial \gamma}{\partial \bar{c}} (1-ZC_o\phi) \quad , \qquad (5.28)$$

where h - fault thickness; γ - the stacking fault free energy; C_o - atomic fraction of solute at the dislocation core.

Estimation of G_B (chemical) using (5.28) (and experimental data on $\partial\gamma/\partial\bar{C}$) for Zn and Ge in Cu gave a value near to 1 KJ/mole (Table 6).

The above discussion leads to a number of conclusions. Firstly, the binding energy ($\Delta G(2r = 3nm) \approx \Delta H$) is lower than ΔH by about two orders. Also, the coefficients of impurity diffusion in the cottrell cloud near dislocations are rather higher than in the matrix solution [75].

Thus, it is impossible to explain the characteristics of the near dislocation segregation phase regions (section 4.2) using the Cottrell cloud model.

5.2 Decoration of Dislocations by a Crystalline Precipitates of the Second Phase

It has long been known that dislocations can act as sites for precipitates of new phases. The precipitates could be either coherent or incoherent with the matrix.

The energy changes associated with these two types of precipitation processes are reviewed. It is further shown that these segregation pahse models are inadequate to explain the diffusion anomalies.

5.2.1 Coherent Precipitation Near Dislocations

In many alloys submitted to an ageing treatment after annealing, precipitation occurs on or near dislocations. In most cases, precipitates on dislocations are likely to be coherent with the matrix, at least in the first stages of precipitation. Accordingly, the precipitation process consists in substituting a number of atoms in the matrix for an equal number of different atoms, which will form the second phase (as illustrated below).

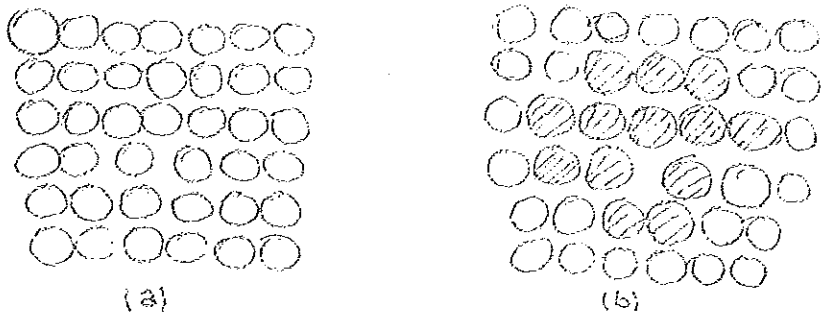

Formation of a coherent precipitate near a dislocation. a) Dislocation without precipitate, b) decorated dislocation. The second phase is constituted here by only one atomic species.

In agreement with numerous experimental observations [76], supported by computer simulations [76,77], it is supposed that the precipitate at any given moment is a cylinder of radius R and of large length that can be taken as infinite. Its axis lies parallel to dislocation line D of an algebriac distance a.

The change ΔE of free enthalpy in the precipitation process was calculated by Montheillet and Haudin [78]. However, the transformation takes place under constant temperature and

pressure and furthermore changes of entropy and volume can be reasonably neglected. Thus, they merely used the energy change $W = W_{DD} - W_D$, where W_{DD} and W_D are the energy of the decorated dislocation and of the dislocation before precipitation, respectively. ΔW is the sum of both elastic and chemical terms.

The formation of a cylinderical coherent precipitate near a dislocation induces a total energy change, taking into account both elastic and chemical energy changes [78]

$$\Delta W = W_{DD} - W_D = W_{\delta'} + W_{\delta} + \Delta W_{SS} + \Delta W_{CH} + W_S \quad , \tag{5.29}$$

where the total change of elastic energy

$$\Delta W_C = W_{\delta'} + W_{\delta} + \Delta W_{SS} \quad , \tag{5.30}$$

and $W_{\delta'}$ and W_{δ} are the parts of the elastic energy corresponding to the modulus effect and to the size effect, respectively. $W_{\delta'}$ and W_{δ} take the following values:

i) dislocation core lying inside the second pahse

$|a| < R - r_c$

$$W_{\delta'} = \frac{\mu_m}{8\pi} B^2 \delta' \log \left(\frac{R^2 - a^2}{r_c^2} \right) \quad , \tag{5.31a}$$

$$W_{\delta} = \frac{2\mu_m}{1+\omega} \left| S^2 \pi R^2 + be \right| \quad ; \tag{5.31b}$$

ii) dislocation core lying inside matrix $|a| > R + r_c$

$$W_{\delta'} = \frac{\mu_m}{8\pi}\,\delta'\left|B^2 \log\left(\frac{a^2}{a^2-R^2}\right) - \frac{3}{4}b_e^2\,\frac{R^2}{a^2}\right| , \qquad (5.32a)$$

$$W_{\delta} = \frac{2\mu_m}{1+\omega}\left|\delta^2\pi R^2 + \delta\, b_e\,\frac{R^2}{a}\right| ; \qquad (5.32b)$$

where

$$\delta' = \frac{\mu_s-\mu_m}{\mu_m} , \quad B^2 = \frac{3}{2}\,b_e^2 + b_s^2$$

$$\delta = \frac{1}{3}\,\frac{V_s-V_m}{V_m} , \omega = \frac{\mu_m}{\lambda_s+\mu_s}$$

μ_m, λ_s, μ_s are the elastic constants of matrix (m) and second phase (s); V_m and V_s the mean atomic volume in the matrix and second phase; b_e and b_s are the edge and screw components of Burgers vector, respectively; r_c is a parameter.

The change of solid solution elastic energy can be calculated by means of the following formula [78]:

$$\Delta W_{SS} = \frac{-\pi R^2}{V_s^2}\,\omega_s , \qquad (5.33)$$

where ω_a is the mean elastic energy of a solute atom in the matrix.

The formation of a second phase involves a change of chemical energy per unit length of precipitate

$$\Delta W_{CH} = \pi R^2 \Delta F , \qquad (5.34)$$

where ΔF is the change of chemical energy per unit volume.

Finally, the interfacial energy W_S between the matrix and the second phase has to be considered

$$W_S = 2\pi R\gamma \quad , \tag{3.35}$$

where γ is the interfacial energy density.

The authors [78] calculated analytically the minimum of ΔW by neglecting the chemical energy terms for an intermetallic compound. Furthermore, they mentioned that the chemical energy terms W_{CH} and W_S are smaller than the elastic energy terms. However, intermetallic compounds have metallic bonds which advance a high chemical energy terms, even greater than the elastic energy terms. Therefore, it is impossible to neglect the chemical energy terms.

On the other hand, Solov'ev [79] have attempted to include the chemical energy terms, but he could not make analytical calculations.

5.2.2 Incoherent Precipitation Near Dislocations

The effectiveness of a dislocation as a catalyst for nucleation was discussed by Chan [80]. Moreover, the author calculated the activation energy for nucleation of a second pahse on a dislocation assuming an elastic model of a dislocation and an incoherent precipitate.

It was assumed, by Chan, that the nucleus lies along the core of the dislocation, that a cross-section of the nucleus

perpendicular to the dislocation is circular. It was further assumed that the nucleus is incoherent with the matrix, that a grain-boundary energy, γ, can be assigned to the boundary between the new phase and the matrix, and that the matrix is an isotropic elastic substance.

The shape of the nucleus is given by the radius $r(z)$, which is a function of distance, z, along the dislocation line. The free energy of formation of a nucleus was found to be [80]

$$\Delta F = \int_{\infty}^{\infty} \Big| - A \log \frac{r}{r_o} + 2\pi\gamma(r\sqrt{1+r'^2} - r_o) - \pi f(r^2 - r_o^2) \Big| dz \quad , \qquad (5.36)$$

where $A = Gb^2/4\pi(1-\nu)$ for edge dislocations and $A = Gb^2/4\pi$ for secrew dislocations, G is the elastic shear modulus, b the Burgers vector; ν the poisson ratio; γ the interfacial energy of the boundary; $f = -\Delta F_v$, the negative of the volume free energy of formation of the new phase (f is a positive quantity when the new phase is stable); r the radius of the nucleus; $r' = dr/dz$ and r_o is given by the minimum in the free energy per unit length

$$F = - A \log r + 2\pi\gamma r - \pi f r^2 + \text{const.} \qquad (5.37)$$

5.2.3 The Diffusion Characteristics in the Segregation Phases

As it is well known, crystaline intermetallic compounds posses metallic bond and have higher melting points, Θ_D (the Debay temperatures) and sublimation heats than their metallic matrices.

According to experimental data and theoretical considerations [81,82] the activation energy of diffusion increases for crystals with higher melting points, Θ_D and sublimation heats (with approximately the same values of D_o). Because of these reasons, at the same absolute temperature T(which is lower than the $T_{m.p}$ of the metallic matrix and much lower than $T_{m.p}$ of the intermetallic compound),

$$Q(\text{in metal}) < Q(\text{in int. comp.})$$

$$D_o(\text{in metal}) \approx D_o(\text{in int. comp.})$$

$$D(\text{in metal}) >> D(\text{in int. comp.})$$

Thus, it is impossible to explain the characteristics of the segregation phase regions (section 4.2) by considering them as crystalline precipitates of intermetallic compounds, since, for the regions, it is necessary to have

$$Q(\text{in metal} > Q(\text{in int. comp.})$$

$$D_o(\text{in metal}) >> D_o(\text{in int. comp.})$$

and $$D(\text{in metal}) >> D(\text{in int. comp.})$$

5.3 "Local Order" Near Lattice Defects

In a series of experimental works [83,84] the concept of the so-called "local order" formations near lattice defects (in particular dislocations) was developed, i.e., the structure and composition of precipitations correspond to short-range order with respect to some compounds. The structure of local order formations is characterized by both individual fragments and inhomogeneous chemical composition and order: microregions with high degree of order alternate with intermediate microzones with relatively low degree or order. In other words such precipitates have structures with some degree of amorphization with respect to the structures of compounds.

As it is shown in the next chapter such a model allows to describe quite satisfactorly the anomalous low characteristic values ($D_{0\perp}$, $Q_{\perp}, D_{\perp}$) in the near dislocation regions, in solutions of transition metals (Fe) in Al.

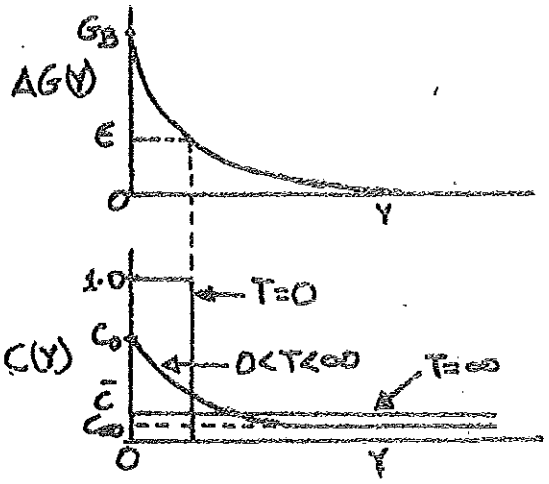

Fig. 7

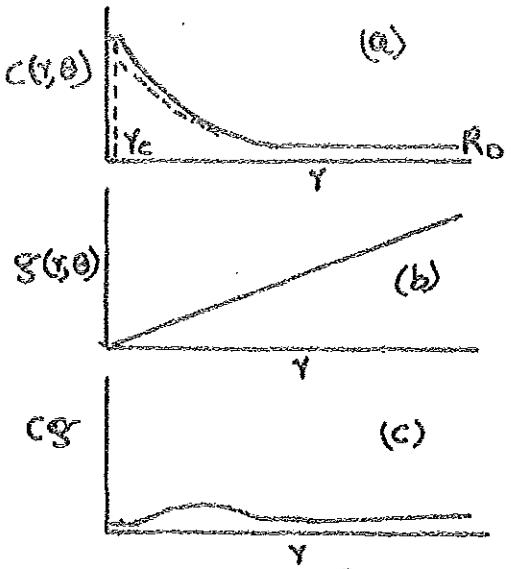

Fig. 8

Fig. 7. Distribution of solute atoms around a dislocation in some arbitrary direction r for various temprutures. Note that the bulk solute concentration ($\bar{c}$) and the solute concentrati when r effectively is equal to infinity ( ) differ by a a small finte amount.

fig 8. Schematic illustrarion (for the case of solute binding) of a) the atomic fraction of solute $c(r,\theta)$ b) the number of sites per unit length of dislocation $g(r,\theta)$ and c) their product, the number of occupied sites per unit length of dislocation, plotted as a function of radial distance from a dislocation and for an arbitrary angle θ. A screened distribution function in a) and the density of solvent plus solute sites in c) are denoted by dashed lines.

TABLE 6

Contributions to the Binding Enthalpy H_B (at $r = b$) of Various Solutes to Edge Dislocations in Dilute Copper Alloys [52]

Binding Enthalpy, H_B KJ/mole	Ni	Zn	Ga	Ge	As
Elastic Misfit	8	13	20	23	32
Elastic Modulus	-3	3	4	6	7
Electrical	0	1	3	5	7
Chemical	-	1	-	1	-
T o t a l	5	18	27	35	46

CHAPTER 6

CONSIDERATION OF DIFFUSION, STRUCTURAL AND THERMODYNAMIC CHARACTERISTICS OF THE NEAR DISOLOCATION SEGREGATION DILUTE SOLUTIONS OF Fe in Al

The existing segregation models, as seen in the preceding chapter, could not explain the near dislocation regions characteristics and the diffusion anomalies. By assuming some degree of amorphization of the intermetallic compound $FeAl_3$ structure, attempt is made to explain the structure and characteristics of the near dislocation regions, thereby interpreting the diffusion anomalies. The linear distribution hypothesis, used in chapter 4, is verified in the light of Crystallography, Thermodynamics and Disolcation theory.

6.1. Interpretation of the Anomalous Low Characteristics of Diffusion of Fe in Al

If the structure of the near dislocations segregation phase region corresponds to a short-range order with respect to some intermetallic compound, for example $FeAl_3$, it is possible to describe the low values of the diffusion characteristics (D_{01}, Q_1 D_1) as follows.

According to the know experimental data and concepts of local order [83-86] its structure could be characterized by both individual fragments and inhomogeneous chemical composition and order: microregions with high degree of

order alternate with intermediate microzones with relatively low degree of order.

It is possible to assume that the composition, structure degree of order (and correspondingly the degree of amorphization) and the cross-sectional diameter of the near dislocations segregation phase regions could vary as a function of the concentration of the impurity (Fe) in the matrix solution (Al). Therefore, the gradient of the chemical potenital of an impurity (Fe), entering the segregation phase regions, may appear along the regions, i.e, under the above conditions. These regions might serve as preferable paths of impurity diffusion or hinder such a diffusion in the bulk owing to depletion of the matrix solution in accordance with the distribution law.

Since the melting point of $FeAl_3$ is rather higher than the melting point of Al, and therefore the melting point of $FeAl_3$ is much higher than the diffusion annealing temperatures of the Al-samples in the experiments [9,12,etc.], it is possible to assume that the diffusion of Fe-atoms in the near dislocation segregation phase regions in Al proceeds preferably along the paths with high diffusion conductivity, i.e, along intermediate microzones with low degree of order.

If the main part of Fe atoms in the near dislocation regions are localized in the microzones with high degree of order, which obviously occupy most part of the regions, then it is possible to describe the effective diffusion

coefficient (D_i) of the impurity in the regions using Hart-Mortlock equation [58]

$$D_i \simeq D_h + D_\ell \eta_\ell K_{\ell h}, \qquad (G.1)$$

where D_h - the diffusion coefficient of the impurity in the microzones with high degree of order;

D_ℓ - the diffusion coefficient of the impurity in the microzones with low degree of order, $D_\ell >> D_h$;

η_ℓ - the fraction of the microzones with low degree of order in the near dislocation regions, $\eta_\ell << 1$;

$K_{\ell h}$ - the equilibrium constant of the process of impurity (Fe) distribution between the microzones with low degree of order and those with high degree of order; $K_{\ell h}\eta_\ell << 1$;

$$K_{\ell h} = \exp(-\Delta S'/R)\exp(\Delta H'/RT), \qquad (6.2)$$

$\Delta H'$ and $\Delta S'$ are changes in enthalpy and entrogy of the system after passing one mole of the impurity atoms from microzones with low degree of order to those with high degree of order.

$$D_h = D_{oh}\exp(-Q_h/RT), \qquad (6.3)$$

$$D_\ell = D_{o\ell}\exp(-Q_\ell/RT), \qquad (6.4)$$

Q_h, Q_ℓ are the activation energies for the impurity diffusion in the microzones with high and low degree of order, respectively ($Q_h > Q_\ell$).

If $D_h << D_\ell \eta_\ell K_{\ell h}$, then

$$D_1 \quad D_\ell \eta_\ell K_{\ell h'} \qquad (6.5)$$

$$D_{o1} \quad D_{o\ell} \eta_\ell \exp(-\Delta S'/R),$$

$$Q_1 \quad Q_\ell - \Delta H'$$

Thus, such a model, with secondary application of Hart-Morflock equation, explains adequately the low values of the diffusion characteristics (D_{o1}, Q_1, D_1) in the near dislocation segregation phase regions of the solutions of transition metals in Al.

In connection with the above statement, it is worthy to consider the $FeAl_3$ crystal chemistry and in particular the possibility of its amorphization in the near dislocation region in Al.

6.2. The Peculiarities of the $FeAl_3$ structure in Near Dislocation Regions in Al.

The $FeAl_3$ structure (space group C2/m) [87,88] could be thought with a certain amorphization of the cubic close-packed lattice of the Al-type. According to Bernal's concepts [89], as interpreted by Pinker [90], the amorphous packing is formed with sufficiently high density of filling, trigonal bipyramides and tetrahedra sharing the faces. These bipyramides and tetrahedra occupy more than half of the $FeAl_3$ structure volume (Fig. 9). Obviously, in this structure some amorphous microregions with no long-range order

(i.e with a short-range order) may occur. For example, such microregions can appear near edge dislocations. Since 3^6 nets correspond to twinning planes Al{111} , the larger fraction of pseudoamorphous regions in $FeAl_3$ structure should make their characteristic nets more similar to Al{ 111 } nets. Therefore, the surface tension at the interface of such microsegregation zones near edge dislocations in Al is lower; the higher is the amorphization degree in this structure.

Characteristic nets of the $FeAl_3$ structure have sites which are potential vacancies ($\square$) with dimensions corresponding to Fe and Al atoms (Fig. 10). For $FeAl_3$ stucture the total number of vacancies per unit cell are about 30. The stochiometric formulae of this compound can be represented, after due consideration of the structural vacancies, as $Fe\square_{1.2}Al_3$ If the $FeAl_3$ structural vacancies are taken into account then the sites form 3^6 nets (Fig. 10) like in close-packed structures(Al). Therefore, the $FeAl_3$ structure can be considered as a quasi-isomorphous structure relative to the Al1 structure. The analysis of the filling density and symmetry relation between the $FeAl_3$ structure and close-packed ones (Al) justify the above assertion.

The above mentioned facts show that the near dislocation formation with structure close to $Fe\square_{1.2}Al_3$ can be considered as quasi-isomorphous stratification of the solution of Fe atoms and vacancies in the dislocation field.

Using such a model it is possible to derive the effective distribution low of Fe atoms between the near dislocation regions and the matrix (Al) solution.

6.3. The Effective Distribution Low of Fe atoms Between the Near Dislocation Segregation Phase Regions and the Matrix (Al) Solution

The $FeAl_3$ (or Fe $\square_{1.2}$ Al_3) structure is more compact than that of Al. Therefore, the segregation phase (Fe $\square_{1.2}$ Al_3) should form in the regions compressive stresses, near edge dislocations where local concentration of Fe atoms and the vacancies is higher [75].

The dissolution "reaction" of the segregation phase in the matrix solution can be represented as

$$(Fe\square_{1.2}Al_3)_{\perp} + 2.2[Al] = [Fe] + 1.2[\square] + 5.2[Al]_{\perp}, \quad (6.6)$$

- -the subscript „$\perp$" indicates "reagent" localized near dislocations in regions with pressure $P_{\perp}$;
- -the square brackets indicate the "reagents" localized in the solution, in the crystal bulk;
- -the square brackets with subscript „$\perp$" indicate „reagent" localized in the solution in the near dislocation regions with pressure $P_{\perp}$;
- - the round bracket with subscript „$\perp$" indicate the stochiometric formula of the near dislocation segregation phase.

The condition of equilibrium for this kind of reaction, from a thermodynamic point of view, can be expressed as [71]:

$$G_{(Fe\square_{1.2}Al_3)_1} + 2.2\,\bar{G}_{[Al]} = \bar{G}_{[Fe]} + 1.2\,\bar{G}_{[\square]} + 3.2\,\bar{G}_{[Al]_1}, \quad (6.7)$$

where $G_{(Fe\ \square_{1.2}\ Al)_1}$ - Gibbs free energy of a mole of the the segregation phase; and all the rest are the partial molar free energies of the „components" in the corresponding solutions.

According to [75, 71]:

$$G_{(Fe\square_{1.2}Al_3)_1} = G^{o}_{FeAl_3} + \Delta G_{am} + (P + \sigma/r)V, \quad (6.8)$$

where $G^{o}_{FeAl_3}$ - the molar free energy of the crystalline compound $FeAl_3$ at atmospheric pressure and given temperture;

ΔG_{am} - the free energy change after amorphization of a mole of the $FeAl_3$ compound of $T > T_{m.p}$.

$$\Delta G_{am} \leq \Delta H \frac{(T_{m.p} - T)}{T_{m.p}}$$

ΔH - the molar melting enthalpy of the compound,

$T_{m.p}$ - the melting point of the compound;

r - the radius of the cross-section of the segregation phase;

σ - the surface tension of the segregation phase-Al interface;

V - V_{FeAl_3} - the molar volume of the segregation phase of P_A and T which can be taken to be equal to the molar volume of $FeAl_3$ at P_A and T.

The partial molar free energies of the „components" can be expressed as [71]:

$$\bar{G}_{[Al]} = G^{o}_{Al} + RT\log(a^{o}_{[Al]}), \tag{6.8}$$

$$\bar{G}_{[Fe]} = G^{o}_{Fe} + RT\log(f^{o}_{[Fe]}\ C_{[Fe]}), \tag{6.9}$$

$$\bar{G}_{[\square]} = RT\log(a^{o}_{[\square]}), \tag{6.10}$$

$$\bar{G}_{(Al]_1} = G^{o}_{Al} + P_1\bar{V}_{[Al]_1} + RT\log(a^{o}_{[Al]_1}), \tag{6.11}$$

where G^{o}_{Al}, G^{o}_{Fe} - the molar free energies of crystalline Al and Fe at atmospheric perssure and T;

$a^{o}_{[Al]}$, $a^{o}_{[\square]}$ - the activities of Al and vacancies in the matrix solution at atmospheric pressure and T;

$C_{[Fe]}$ - the concentration (in atomic fraction) of Fe atoms in the matrix (Al) solution at atmospheric pressure and T;

$f^{o}_{[Fe]}$ - the coefficient of the activity of Fe atoms in the matrix (Al) solution at atmospheric pressure and T;

$a^{o}_{[Al]_1}$ - the activity of Al atoms in the solution in the near dislocation regions at atmospheric pressure and T;

$\bar{V}_{[Al]}$ - the partial molar volume of Al in the solution in the near dislocation regions of P and T, which cab be taken to be equal to the molar volume of crystalline Al at P_1 and T ($\bar{V}_{[Al]} = V_{Al}$).

The coefficient of activity of Fe atoms in dilute matrix

solution can be represented as [71]:

$$f^{o}_{[Fe]} = \exp\left(\frac{\Delta\bar{H}_{[Fe]}}{RT}\right) \exp\left(\frac{\Delta\bar{S}^{E}_{[Fe]}}{R}\right), \qquad (6.12)$$

wher $\Delta\bar{H}_{[Fe]}$ - the relative partial molar enthalpy of Fe atoms in the Al matrix solution;

$\Delta\bar{S}^{E}_{[Fe]} = \Delta\bar{S}_{[Fe]}$ - the excessive partial molar entropy of Fe atoms in Al matrix solution which can be taken to be equal to the relative partial molar entropy ($\Delta\bar{S}_{[Fe]}$)

When the crystal is in equilibrium with its surface $a^{o}_{[\square]} = 1$ [71] and in a good approximation $a^{o}_{[Al]} = 1$ and $a^{o}_{[Al]} = 1$ as well. Hence the expression for Fe concentration (in atomic fraction) in the matrix (Al) solution saturated with respect to segregation phases on dislocations at T can be obtained as:

$$C^{s.ph}_{[Fe]} = \exp\left\{\frac{\Delta G^{o}_{FeAl_3} + \Delta G_{am} + P\ \Delta V + \frac{\Delta V_{FeAl_3}}{r} + \Delta G_{[Fe]}}{RT}\right\}, \qquad (6.13)$$

where $G^{o}_{FeAl_3} = (G^{o}_{FeAl} - G^{o}_{Fe} - 3G^{o}_{Al})$ is the standard free energy of the formation of a mole of crystalline $FeAl_3$ from crystalline Al and Fe at T;

$$\Delta G^{o}_{FeAl_3} = \Delta H^{o}_{FeAl_3} - T\,\Delta S^{o}_{FeAl_3}, \qquad (6.14)$$

$\Delta H^{o}_{FeAl_3}$, $\Delta S^{o}_{FeAl_3}$ are the standard enthalpy and entropy of the formation of a mole of crystalline $FeAl_3$ from crystalline Al and Fe at T;

$$G_{am} \leq H_{am}\left(1 - \frac{T}{T_{m.p}}\right),$$

$$\bar{G}_{[Fe]} = \bar{H}_{[Fe]} - T\,\bar{S}_{[Fe]},$$

$$\Delta V = V_{FeAl_3} - 5.2\,V_{Al}$$

The pressure of uniform compression P in the stress field of an edge dislocation, in the solution of Fe in Al, can be estimated in the framework of the isotropic continuum approximation [75]:

$$P_{\perp} = \frac{\mu b(1+x)}{6\pi(1-x)}\,\frac{1}{r} = \frac{A}{r}, \qquad (6.15)$$

where μ- the shear modulus (Al), b-the Burgers vector(Al) and x-poisson's ration (Al).

In this approximation, surfaces of constant pressure ($P_{\perp}$) are cylinders (with radius r) tangent to the glide plane along the dislocation line, the pressure decreasing inversely with the cylinder radius (Eq. (6.15)). The shape of the cross-section of the near dislocation segregation phase can be approximated by the contour of constant pressure of uniform compression.

Assuming $r \simeq 1.5$ nm (since the diameter of the near dislocation segregation regions is about 3nm), b = 0.286nm[75], $\mu = 2.65 \times 10^{11}$ dynes/cm^2 [75], $x = 0.347 \times 10^{11}$dynes/cm^2 [75]; thus $P_{\perp}$ ($r \simeq 1.5$nm) $\simeq 5 \times 10^{8}$ P_a. Taking the value [87, 88, 91, 92] $\Delta V \simeq 15 \times 10^{-6}$ $\frac{m^3}{mole}$, hence $P_{\perp}\Delta V \simeq 8$KJ/mole.

At high temperatures, close the $T_{m.p}$ of Al, the ΔG_{am} term can be neglected. In accordance to section 6.2, the

crystallographic consideration, the value of σ is rather small. For example, $\sigma = 10^{-2}$ N/m (for coherent twin boundaris). Taking $\sigma = 10^{-2}$ N/m, r = 1.5 nm and V_{FeAl_3} 37.3 x 10^{-3} m^3/mole [87, 88, 91, 92]; then

$$\frac{\sigma V_{FeAl_3}}{r} = 2.5 \times 10^2 \text{ J/mole}$$

Also, $\Delta H^{o}_{FeAl_3} \simeq -112.4$ KJ/mole and $\Delta S^{o}_{FeAl_3} \simeq -15.8$ J/mol.k [92]

In order to estimate $\Delta\bar{H}_{[Fe]}$ and $\Delta\bar{S}_{[Fe]}$ the process of dissolution of macroscopic crystalline particles of of $FeAl_3$ in Al-lattice at high temperature could be considered:

$$(FeAl_3) = [Fe] + 3[Al]$$

From the view of the thermodynamic condition of equilibrium of the corresponding "reaction", within the framework of the thermodynamic theory of dilue solutions, the following expressions can be obtained:

$$C^{(FeAl_3)}_{[Fe]} \simeq \exp(\Delta S/R)\exp(-\Delta H/RT), \qquad (6.16)$$

$$\Delta H = \Delta\bar{H}_{[Fe]} - \Delta H^{o}_{FeAl_3}, \qquad (6.17)$$

$$\Delta S = \Delta\bar{S}_{[Fe]} - \Delta S^{o}_{FeAl_3} \qquad (6.18)$$

where $C^{FeAl_3}_{[Fe]}$ is the iron concentration (in atomic fraction) in the matrix(Al) solution saturated with respect to the macroscopic crystalline particles of $FeAl_3$ at T; ΔH, ΔS are the enthapiy and entropy of dissolution of $FeAl_3$ in Al. According to experimental data [63, others].

$$\Delta H = 62.7 \pm 1.7 \text{ KJ/mole},$$

$$\Delta S = (2.3 \pm 0.3)R = (19.1 \pm 2.5) \text{J/mole.K}.$$

Hence

$$\Delta\bar{H}_{[Fe]} = \Delta U + \Delta H^{o}_{FeAl_3} = -29.7 \pm 2 \text{ KJ/mole}$$

and

$$\Delta\bar{S}_{[Fe]} = \Delta S + \Delta S^{o}_{FeAl_3} = 3.3 \pm 1.5 \text{ J/mole.K}$$

Eqs.(6.13) and (6.16) lead to

$$C^{S.ph}_{[Fe]} / C^{FeAl_3}_{[Fe]} \approx \exp\left\{\frac{\Delta G_{am} + (\sigma V_{FeAl_3}/r) + P_{\perp}\Delta V}{RT}\right\} < 1, \quad (6.19)$$

since $\{\Delta G_{am} + (\sigma V_{FeAl_3}/r) + P_{\perp}\Delta V\} < 0$

It indicates that the segregation phases on dislocation appear earlier than the macroscopic crystalline $FeAl_3$ particles (in the matrix solution) do.

Thus, the thermodyanmic stability of the segregation phases on dislocations in Al solution is unsaturated, with respect to crystalline $FeAl_3$ phase, mainly due to the dilametric effect ($P_{\perp}\Delta V<0$) segregation phases - Al interface.

As it was shown above:

$$H = (\Delta\bar{H}_{[Fe]} - \Delta H^{o}_{FeAl_3}) >> |\Delta G_{am} + \sigma V_{FeAl_3}/r + P_{\perp}\Delta V|. \quad (6.20)$$

Hence, in satisfactory approximation

$$C = C^{S.ph}_{[Fe]} \approx C^{(FeAl_3)}_{[Fe]} \approx \exp(-\Delta H/RT). \quad (6.21)$$

The effective distribution low can be represented as

$$\frac{N_{\perp}}{C} = \frac{N\Sigma - C}{C} \approx \eta_{\perp} K_{\perp}$$

where $N_{\perp} = C\ \eta_{\perp} >> C$

$N_{\perp} + C = N\Sigma$ - the total atomic fraction of the impurity(Fe) in the system.

Then

$$\frac{N_\perp}{C} \approx \frac{N_\Sigma}{C} \approx \eta_\perp K_\perp$$

hence

$$\eta_\perp \approx N_\Sigma$$

and $$K_\perp \sim \frac{1}{C} \sim \exp\ (\Delta_H/RT),$$

i.e $$K_\perp \sim \exp(\Delta_H/RT)$$

Thus, in the framework of the model, the effective distribution law corresponds to a linear concentration dependence, and the effective binding energy of the impurity atoms (Fe) to the near dislocation regions(in Al) is close to enthalpy of dissolution of the intermetallic compound ($FeAl_3$) in the Al matrix in agreement with the results of the treatment of the experimental data on the anomalous diffusion characteristics.

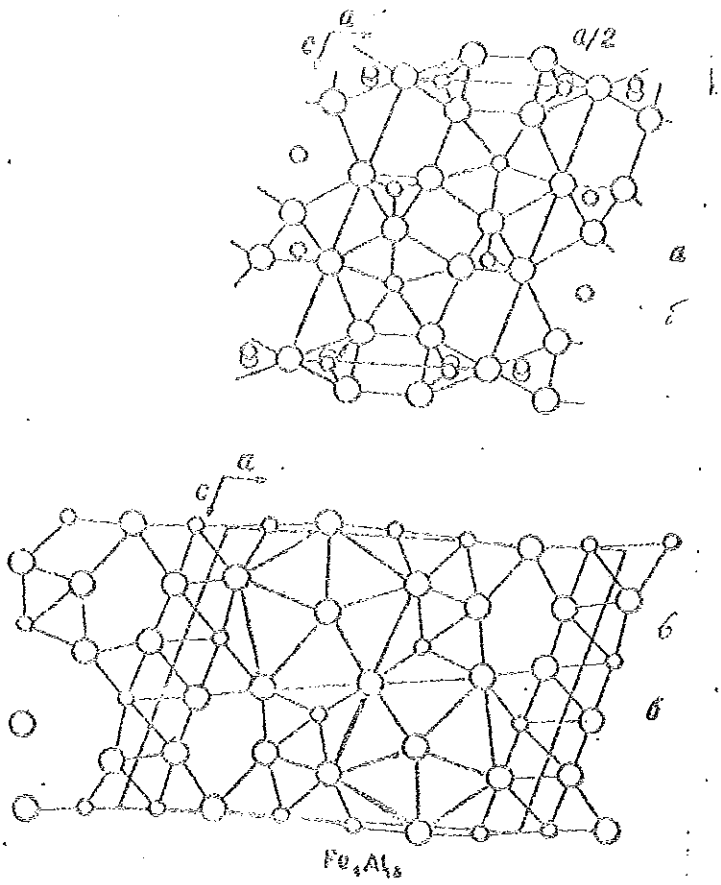

Fig.9. The $FeAl_3$ structure in the projection along [010]
Positions of Bernel's triagonal bipyramides and tetrahedra in $FeAl_3$ structure are shown.

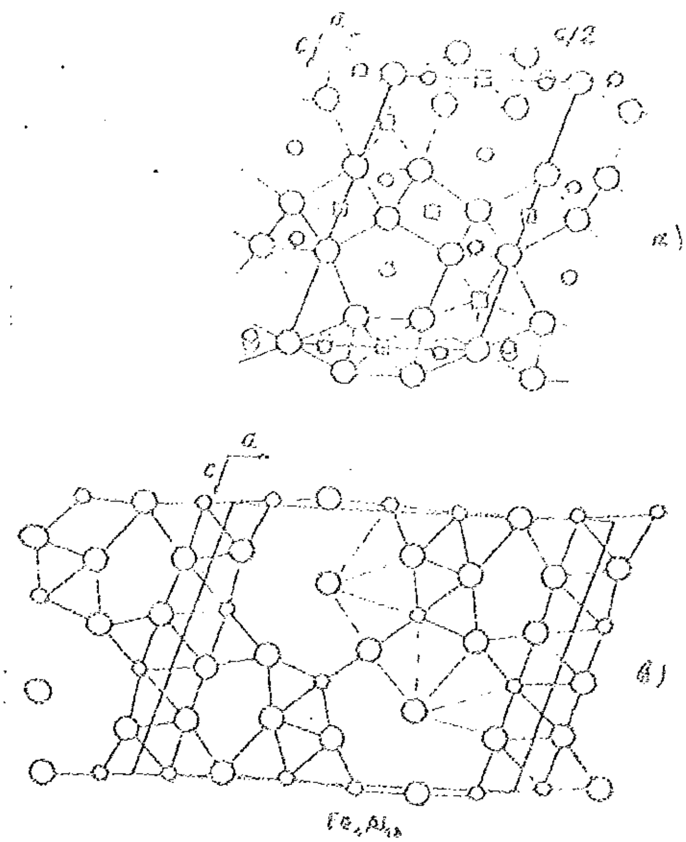

Fig 10. The structure of $FeAl_3$ (C2/m) in the projection along [010]

a) Flat nets $5^2 4 3 + 5 4 3 4$

b) Puckered nets with regions $3^4 5$ and 3^5
O–Al, ⊗ o–Fe, □ –Vacancy. The ~ sign shows the regions which is isomorphous to nets 3^6(Al).

RECOMMENDATIONS

1. The near dislocation segregation phases in solutions of Fe in Aℓ can be studied by gamma-resonance spectroscopy. To determine thermodynamic characteristics of the process of the formation of segregation pahses near dislocation in solutions of Fe in Aℓ unsaturated with respect to the $FeAℓ_3$-phase a special procedure can be used which is based on measuring Mossbauer (absorption) spectra of quenched samples. The intensity of the lines due to the segregation phases should increas with growth of $\rho_{\perp}$, while that due to the bulk solution should decrease, and the intensity of the lines due to the segregation phases should decrease with growth of the quenching temperature while that of the bulk solution should increase.

2. The true volume diffusion characteristics of transition metal impurities in Aℓ can be measured under conditions of plastic deformation or in very dilute solutions where there is no segregation phases on dislocations by using Mossbauer method.

CONCLUSION

The experimental observations of different investigators indicate that transition impurities diffuse in Al with three distinct family of characteristics. On of which, normal characteristics, have been explained by the well established LeClaire-Lazarus model. But the anomalous high and low characteristics have not been interpreted inspite of the multiform attempts.

Experimental reports indicated that in the near surface zone high dislocation density is manifested. In addition, due to the low solubility of transition impurities in Al segregation phases are modelled. Assuming the corresponding working hypotheses, based on the experimental data analysis, attempt was made, in this paper, to interprete the transition impurity diffusion anomalies in Al.

The simple theoretical model developed based on the experimental observations of different investigators has proved to be capable of interpreting the transition impurity diffusion anomalies in Al. Using this theoretical model, the various experimental data were treated, thereby indicated the near dislocation segregation phase characteristics. For proper and complete theoretical description of the anomalies characteristics the corresponding segregation phase model was developed (since the existing segregation.(Cottrel cloud) and segregation phases (precipitates) were inadiquite) which was found to be the corresponding intermetallic compound with a certain degree of amorphization.

The present work showed that the normal diffusion of transition impurity characterize the true volume diffusion. The remaining two, the anomalous high and low characteristics, were obtained due to the influence of dislocations decorated by segregation phases. All are equally important results and valied. Thus, one has no ground to discard two of them (say normal and low) and consider one of which (high) as the true volume diffusion.

Eventhough the developed theoretical model was based on the experimental observations, it needs further experimentation. The accompaning segregation phase model require further experimental study which is beyond the limits of this thesis.

REFERENCES

1. e.g. Smithells, C.J. (Ed.). Metals Reference Book. Fifth edition. London: Butterworths and Company, Ltd., 1976.

2. Le Claire, A.D. Solute Diffusion in Dilute Alloys, Journal of Nuclear Materials, 1978, 69: 70-97.

3. Bokstein, B.S. "Diffusion in Metals". Moscow: Metallurgy Publisher, 1978 (In Russian).

4. Beyer, M. and Adda, Y. Determination des Volumes d'activation pour la diffusion des atoms dans l'or, le cuivre et l'aluminium, Journal de Physique, 1968, 29: 545-552.

5. Lundy, T.S. and Murdock, J.F. Diffusion of Al^{26} and Mn^{54} in Aluminium, Journal of Applied Physics, 1962, 33: 1671-75.

6. Peterson, N.L. and Rothman, S.J. Impurity Diffusion in Aluminium, Physical Review B., 1970, 1: 3264-74.

7. Anand, M.S. Murarka, S.P. and Agrarwala, R.P. Diffusion of Copper in Nickel and Aluminium, Journal of Applied Physics, 1965, 36: 3860-62.

8. Alexander, W.B. and Slifkin, L.M. Impurity Diffusion in Aluminium, Physical Review B., 1970, 1: 3274-82.

9. Hirano, K. Diffusion in Aluminium. "The Proceedings of International Symposium on Fifty Years of Metallurgy", Banaras Hindu University, varanasi. The Indian Institute of Metals. Calcutta, 1973, pp. 237-58.

10. Hirano, K. and Fujikawa, S. Impurity Diffusion in Aluminium, Journal of Nuclear Materials, 1978, 69(70): 564-66.

11. Rothman, S.J. et.al. Tracer Diffusion: Magnesium in Aluminum Single crystals, Physica Status Solidi b. 1974, 62:29-33.

12. Hood, G.M. and Schultz, R.J. Indium Diffusion in Aluminium, Physical Review B, 1971, 4: 2339-41.

13. Hillard, J.E., Averbach, B. and Cohen, M. Self- and Inter-diffusion in Aluminium-zinic Alloys, Acta Metallurgica, 1959, 7: 86-92.

14. Bergner, D. and Cyrener, E. Diffusion Von Fremdelementen in Aluminium-Mischkistallen, Neue Hutte, 1973, 18: 356-61

15. Anand, M.S. and Agarwala, R.P. Effect of the Oxide Method on Impurity Diffusion in Aluminium, Physica Status Solidi a, 1970, 1: 41-43.

16. Bandrinarayanan, S. and Mathus, H.B. Impurity Diffusion of Antimony and Silver in Aluminium, International Journal of Applied Radiation and Isotops, 1963, 19: 353-60

17. Hood, G.M. and Schultz, R.J. The Diffusion of Manganes in Aluminium, Philosphical Magazine, 1971, 23: 1479-89.

18. Fricke, W.G. Diffusion in Aluminium. Edited by Van Horn K.R. Ohio: American Society for Metals Park, 1967, 1: 250.

19. Hood, G.M. The Diffusion of Iron in Aluminium, Philosopical Magazine, 1970, 21: 305-28.

20. Agarwala, R.P., Murarka, S.P. and Anand, M.S. Diffusion of Chromium in Aluminium, Acta Metallurgica, 1964, 12: 871-75.

21. Anand, M.S. and Agarwala, R.P. Diffusion of Cobalt in Aluminium, Philosophical Magazine, 1972, 26: 297-309.

22. Patial, R.V. and Tiwari, G.P. Diffusion of Cobalt in Aluminium, Transactions of Indian Institute of Metals, 1974, No. 4, 27: 215-20.

23. Murarka, S.P., Anand, M.S. and Agarwala, R.P. Diffusion of Vanadium in Aluminium and Nickel, Acta Metallurgica, 1968, 16: 69-72.

24. Anand, M.S. and Agarwala, R.P. Diffusion of Palladium, Silver, Cadmium, Indium and Tin in Aluminium, Transactions of the Metal Society AIME, 1967, 239: 1848-55.

25. Paul, A.R. and Agarwala, R.P. Diffusion of Molybdenum in Aluminium, Journal of Applied Physics, 1967, 38: 3790-91.

26. Tiwari, G.P. and Sharma, B.D. Diffusion of Nb in Al, Transactions of Indian Institute of Metals, 1967, 20: 85-88.

27. Le Claire, A.D. Physical Chemistry. An Advanced Treatise Academic Press, Vol. 5 (Chapter 5), 1970.

28. Le Claire, A.D. On the Theory of Impurity Diffusion in Metals, Philosopical Magazine, 1962, 7: 141-67.

29. Lazarus, D. Effect of Screening of solute Diffusion in Metals, Physical Review, 1954, 93: 973-76.

30. Alfred, L.C.R. and March, N.M. Impurity-vacancy Interaction in a Metal, Philosophical Magazine, 1957, 2: 985-97.

31. Umeda, K. and Kobayashi, J. Impurity Diffusion in Metals, Journal of Physical Society of Japan, 1958, 13: 148-153.

32. Le Claire, A.D. and Lidiard, A.B. Philosopical Magazine, 1956, 1: 518.

33. March, N.H. Point Defect-Solute Interactions in Metals, Journal of Nuclear Materials, 1978, 69 (70): 490-520.

34. Kohn, W. and Vosko, S.M. Theory of Nuclear Resonance intensity in Dilute Alloys, Physical Review, 1960, 119: 912-918.

35. Langer, J.S. and Vosko, S.H. The Shielding of Fisced Charge in a High Density Elector Gas, Journal of Physics and and Chemistry of Solids, 1960, 12: 196-205.

36. Blandin, A.P. and Deplante, J.L. Effect de Taille et Interactions Chimiques dus dux Impuretes de Transition dans Les Metaux Normaux, The Physics and Chemistry of Solids, 1965, 26: 381-89.

37. Blandin, A.P. and Friedel, J.J. Effects Quadrupolaires dans la de Resonanse Magnetique Nucleaire des Alliages Dilues, J.de Physique et le Radium, 1960, 21: 689-95.

38. March, N.H. and Murray, A.N. Relation Between Dirac and Canonical Density Matrics with Applications to Imperfection Metals, Physical Review, 1960, 120: 830-36.

39. March, N.H. and Murray, A.N. Self-consistent Perturbation Treatment of Impurities and Imperfections in Metals, Proceedings of Royal Society A, 1961; 261: 119-30.

40. Swallin, R.A. A Model for Solute Diffusion in Metals Base on Elasticity Concepts, Acta Metallurgica, 1957, 5:

41. Seeger, A. Investigation of Point Defects in Equilibrium Concentrations with Particular Reference to Position Anhilation Techniques, Journal of Physics F Metal Physics, 1973, 3: 248-94.

42. Miki, I. and Warlimont, H. Morphology and Kinetics of Precipitation Processes in Aluminium-Rich Al-Fe-and Al-Fe-Si Alloys, Z. Metallkde, 1968, No. 4, 59: 254-64, 408-14 (in German).

43. Stickels, C.A. and Bush, E.A. Precipitation in the System Al-0.05 wt.pct. Fe, Metallurgical Transactions, 1971, 2: 2031-42.

44. Sorenson, K. and Frumpy, G. Dinamical Properties of ^{57}Fe D Disolved in Al observed by Mossbauer Effect, Physical Review B, 1973, 7: 1891-97.

45. March, N.H. and Rousseau, J.S. Interaction Between Point Defects in Metals, Crystal Lattice Defects, 1971, 2: 1-46.

46. Coriess, G.K. and March, N.H. Saddle-Point Configuration in Impurity Diffusion in Face-centred cubic Metals, Philosophical Magazine, 1962, 7: 1769-72.

47. Yamamoto, R., Dayama, M. and Takai, O. The Effect of Impurities on Diffusion in Metals, Physics Letters, 1973, 44A: 105-06.

48. Takai, O. et.al. Migration Energies of Impurity Atoms in Cubic Metals, Journal of Physics F Metal Physics, 1975, 5: 183-186.

49. Du Charme, A.R. and Straul, C.K. On the Diffusion of Divalent Impurities in Aluminium, Physica Status Solidi b, 1975, 69: 23-27.

50. Kisilishin, V.A. "On Relationship Between Do and Q for Diffusion in Crystals", Metals, Proceedings of Academy of Science (USSR), 1976, No. 1, pp. 230-33.

51. Swalin, R.A. Correlation Between Frequency Factor, Journal of Applied Physics, 1956, 27: 554-55.

52. Friedel, J. "Dislocations". New York: Pergamon, 1964.

53. Massalski, T.B. Physical Metallurgy, Chan, R.W., editor. Amsterdam: North Holland Publishing Company, 1965.

54. Huntington, H.B., Shirn, G.A. and Wajda, E.S. Calculation of the Entropies of Lattice Defects, Physical Review, 1955, 99: 1085-91.

55. Wynblatt, G. On the Formation and Migration Entropies of Vacancies in Metals, Journal of Physics and Chemistry of Solids, 1969, 30: 2201-11.

56. Hart, E.W. On the Role of Dislocations in Bulk Diffusion, Acta Metallurgica, 1957, 5: 597.

57. Balluffi, R.W. On dislocation Short-circuiting Models for Recently Observed Diffusivities of Iron, Nickel and Cobalt Solutes in Aluminium, Acta Metallurgica, 1963, 11: 1109-11.

58. Mortlock, A.J. The Effect of Segregation on the Solute Diffusion Enhancement due to the Presence of Dislocations, Acta Metallurgica, 1960, 8: 132-33.

59. Mortlock, A.J. Anomalous Volume Diffusion in the Surface Layers of Metals, Acta Metallurgica, 1964, 12: 675-77.

60. Tiwari, G.P. and Sharma, B. D. Diffusion of Iron in Aluminium, Philosophical Magazine, 1971, 24: 739-43.

61. Bolfoks, B.I. Diffuziya i tochechnye defekty poluprovodinkakh (Diffusion and Point Defects in Semiconductors). Moscow: Nauka, 1972 (in Russian).

62. Friedel, J. "Les Dislocations". Paris: Gauthiers-villaris, 1956 (in French).

63. Edger, J.K. Metal Transaction, 1949, 180: 225

64. Hordon, M.J. and Averbach, B.L. X-Ray Measurements of Dislocations Density in Deformed Copper and Aluminium single crustals, Acta Metallurgica, 1961, 9: 237-46.

65. Cottrell, A.H. Report of A Conference on Strength of Solids. London: The Physical Society, 1948, p. 30.

66. Nabarro, F.R.N. Report of a Conference on Strength of Solids. London: The Physical Society, 1948, p. 38.

67. Fiore, N.F. and Bauer, C.L. Binding of Solute Atoms to Dislocations, Progress in Material Science, 1968, 13: 87-134.

68. Davis, C.K.L., Davis, P.W. and Wilshire, B. The Effect of Variations in Stocking-Fault Energy on the Creep of Nickel-Cobalt Alloys, Philosopical Magazine, 1965, 12: 827-39.

69. Bauer, C.L. The Binding Entropy of Point Defects to Dislocations, Journal of Physics and Chemistry of Solids, 1966, 27: 1133-37.

70. Fisher, J.C. On the Strength of Solid Solution Alloys, Acta Metallurgica, 1954, 2: 9-11.

71. Swalin, R.A. Thermodynamics of Solids. Second Edition. New York: John Wiley & Sons, 1972.

72. Fleischer, R.L. Solution Hardening, Acta Metallurgica, 1961, 9: 996-1000.

73. Cottrel, A.H., Hunter, S.C. and Nabarro, F.R.N. Electrical Interaction of Dislocation and a solute Atome, Philosopical Magazine, 1953, 44: 1064-67.

74. Suzuki, H. Sergregation of Solute Atoms to Stacking Faults, Journal of Physical Society of Japan, 1962, 17: 322-25.

75. Hirth, J.P. and Lothe, J. Theory of Dislocations. New York: McGraw Hill Book Company, 1968.

76. Haudin, J.M. and Montheillet, F. Electron Microscope Study of Precipitation Hardening in the Ferrite of a Stainless Steel (Cr 15%, Ni 7%, No 2%), the Precipitation of the R Phase, Metallography, 1978, 11: 391-428.

77. Montheillet, F., Haudin, J.M. and Frade G. Electron Microscope study of the Contrast of Decorated Dislocations in some Cubic Structures, Physica Status Solidi a, 1973, 17: 593-607.

78. Montheillet, F. and Haudin, J.M. Coherent Precipitations Near Dislocations, Physica Status Solidi a, 1979, 54: 271.

79. Solov'ev, V.A. FTT (Physics of Solid State), 1978, 20:775 (in Russian).

80. Chan, J.W. Nucleation on Dislocations, Acta Metallurgica, 1957, 5: 169-71.

81. Larikov, L.N. "avtomficheskj savarka", 1971, No. 24 (in Russian).

82. Larikov, L.N. et.al. "Zaschcta Metallov", 1970, No. 24 (in Russian).

83. Iveronova, V.I. et.al. Specific Features of Local Distributions of Atoms in Cu-Pt Alloys, Fiz. Metallov and Metalloyed (USSR). English Translation: Physics Metals and Metallography, 1973, No. 2, 35: 118-125.

84. Katsnel'son, A.A. et.al. Local ordering and Electrical Resistance of Ni-W and Pd-Co Alloys, Fiz. Metalloy Metallovedenie (USSR). English Translation: Physics Metals and Metallography, 1968, No. 6, 26: 26-35.

85. Iveronova, V.I. and Katsnel'son, A.A. Short-range Order in Solid Solutions. Moscow: Nauka, 1977 (in Russian).

86. Iveronova, V.I. and Katsnel'son, A.A. Izvestigay Vuzov, Fizika, 1978, No. 8, pp. 40-52 (in Russian).

87. Peterson, W.B. The Crystal Chemistry and Physics of Metals and Alloys. New York: McGraw Hill Book Company, 1972.

88. Black, J. The Structure of $FeAl_3$ I and II, Acta Crustallography, 1953, 8: 43-48, 175-82.

89. Bernel, J.D. The Bakerian Lecture, 1962, The Structure of Liquids, Proceedings of the Royal Society, 1964, 280A: 299-322.

90. Pinker, G.Z. Neorganichesinic Materialy, Izv. AN SSSR, 1979, No. 10, 15: 171 (in Russian).

91. Bridgmen, P.W. Collected Experimental Papers, Cambridge (mass), 1964, 3: 43-45.

92. Robinson, P.M. and Bever, M.B. Thermodynamic Properties of Intermetallic Compounds, Intermetallic Compounds. Editor Westbrook, J.H.

DECLARATION

I hereby declare that the thesis entitled, "The Analysis and Interpretation of the Anomalies Transition Impurity Diffusion in Aluminium", being submitted by me in partial fulfillment for Master of Science Degree in Physics, is my original work, done under the supervision and guidance of Dr. J. Netchaev. All sources of relevant findings and materials used for the thesis have been duly acknowledged.

Yewondwossen Mammo

This Thesis has been submitted for examination with my approval as University Advisor.

J. Netchaev, Ph.D.